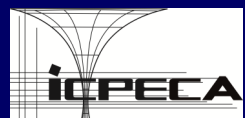




BULLETIN of MICRO and NANOELECTROTECHNOLOGIES

ISSN 2069-1505



National Institute for R&D in Electrical
Engineering ICPE-CA Bucharest
INCDIE ICPE-CA

Address:

313 Splaiul Unirii, District 3, Bucharest—030138, Romania

Phone: +40-21-346.72.31, 021-346.72.35

Fax: +40-21-346.82.99

E-mail: editura.icpe-ca@icpe-ca.ro

<http://www.icpe-ca.ro/vizibilitate/publicatii-2/reviste-interne/buletin-of-micro-and-nanoelectrotechnologies/>

BUCHAREST

2022

EDITOR IN CHIEF
Dr. Eng. Mircea IGNAT

EXECUTIVE STAFF
Dr. Eng. Cristian MORARI

Editorial secretary
Technical editing, graphic design and layout
Eng. Gabriela OBREJA

Brochure binder
Matilda GHEORGHIU

Webmaster
Dr. Eng. Dorian MARIN

PUBLISHER: INCDIE ICPE-CA Bucharest

Address:

313 Splaiul Unirii, District 3, Bucharest—030138, Romania

Phone: +40-21-346.72.31, 021-346.72.35

Fax: +40-21-346.82.99

E-mail: editura.icpe-ca@icpe-ca.ro

Contact Person: Dr. Eng. Mircea Ignat - INCDIE ICPE-CA

E-mail: mircea.ignat@icpe-ca.ro, mobil 0755.015.606

ISSN 2069-1505

Bulletin of Micro and Nanoelectrotechnologies

Editorial Board

Scientific Staff

- Alexandru ALDEA** – National Institute of Material Physics, Bucharest, Romania
- Robert Allen** - University of Southampton, UK
- Leonardo G. ANDRADE E SILVA** - Institute for Nuclear Energy Research, Av. Prof. Lineu Prestes, São Paulo, Brazil
- Ioan ARDELEAN** - Academy Romanian Institute of Biology, Bucharest, Romania
- Marius BĂZU** – National Institute for R&D in Microtechnologies, Bucharest, Romania
- Constantin BREZEANU** - Faculty of Electronic, University Politehnica of Bucharest, Romania
- Maria CAZACU** – “Petru Poni” Institute of Macromolecular Chemistry of Romanian Academy, Iassy, Romania
- Mircea CHIPARĂ** - The University of Texas Pan American, Physics and Geology Department, USA
- Sorin COȚOFANĂ** - The Deft University, The Netherland
- Olgun GÜVEN** - Hacettepe University, Department of Chemistry, Polymer Chemistry Division, Ankara, Turkey
- Elena HAMCIUC** – “Petru Poni” Institute of Macromolecular Chemistry of Romanian Academy, Iassy, Romania
- Wilhelm KAPPEL** - INCDIE ICPE-CA, Bucharest, Romania
- Yoshihito OSADA** - Hokkaido University, Riken Advanced Science Institute, Japan
- Mircea RĂDULESCU** – Technical University of Cluj-Napoca, Romania
- Yoshiro TAJITSU** - Kansai University, Japan
- Cristian TEODORESCU** - National Institute of Material Physics, Bucharest, Romania
- Elena TRIF** – Institute of Biochemistry of Romanian Academy, Bucharest, Romania
- Traian ZAHARESCU** – INCDIE ICPE-CA, Bucharest, Romania
- Slawomir WIAK** - Technical University of Lodz, Poland

Executive Staff

- Cristian MORARI** - INCDIE ICPE-CA, Bucharest, Romania
- Gabriela OBREJA** - INCDIE ICPE-CA, Bucharest, Romania

Editor in chief

PhD. Eng. Mircea IGNAT - INCDIE ICPE-CA, coordinator of the “Alexandru Proca” Centre for the Youngsters Initiation in Scientific Research (CITCS), mircea.ignat@icpe-ca.ro

ISSN 2069-1505

Manuscript submission

The Guest Editors will send the manuscripts by post or to the e-mail: mircea.ignat@icpe-ca.ro

Address:

Splaiul Unirii No. 313, sect. 3, Bucharest – 030138, Romania

Our staff will contact the Guest Editors in order to arrange future actions concerning manuscripts.

Bulletin of Micro and Nanoelectrotechnologies includes the specific research studies on:

- Microelectromechanical and nanoelectromechanical components;
- The typical micro and nanostructure of actuators, micromotors and sensors;
- The harvesting microsystems;
- The conventional and unconventional technologies on MEMS and NEMS;
- The theoretical and experimental studies on electric, magnetic or electromagnetic field with applications on micro and nano actuating and sensing effects;
- The design algorithms or procedures of MEMS and NEMS components;
- The applications of MEMS and NEMS in biology and in biomedical field;
- The new materials in MEMS and NEMS;
- The standardization and reliability preoccupations;
- The economic and financial analysis and evolutions of MEMS and NEMS specific markets.

CHRONICLE

The 3-4/2022 number of Bulletin of Micro and Nanoelectrotechnologies includes three papers: two papers dedicated to the mathematics applications (which belong to Victor Eduard Albei, member of the Alexandru Proca Center and “Tudor Vianu” National College of Informatics, Bucharest), and a paper dedicated to the theoretical aspects of ponderomotive forces.

Also, we mention the qualification of 4 projects of the Alexandru Proca Center to the very important research projects competition ISEF 2022, Atlanta - USA, 7-13 May:

- *Green Interpenetrated III. Silicone-Based Elastomeric Webs Engineered as Wave Energy Harvesters* - **Natalia Ionescu**, 18, “Mihai Viteazul” National College, Bucharest;
- *Guidance system for the visually impaired* - **Mihai Dumitrescu**, 17, International Theoretical High School of Informatics, Bucharest, **Mihai Vârlan**, 17, “Mihai Viteazul” National College, Bucharest, **Matei Iosip**, 17, Hermann Oberth German School, Bucharest;
- *Applications of Electromagnetic Forces in Medicine* - **Cristiana Andreea Murgoci**, 18, International Theoretical High School of Informatics, Bucharest;
- *Demyelinating: a Research into the Use of Electrical Models in Studying Demyelinating Diseases* - **Despina Gica**, 18, “Mihai Viteazul” National College, Bucharest.

On 15th June, we had the Research Communication Session of the Alexandru Proca Center.

Editor in Chief,

Dr. Mircea Ignat

Contents

Explained Usage of Quaternions and Transformation Matrices in the Development of a Computer-Assisted Pilot Helmet Victor-Eduard Albei	7
Description of the Fourier Transform and the Development of an Audio-Based Replacement for the RS-232 Standard Victor-Eduard Albei	19
Theoretical Aspects on Ponderomotive Forces Mircea Ignat	33

Explained Usage of Quaternions and Transformation Matrices in the Development of a Computer-Assisted Pilot Helmet

Albei Victor-Eduard

“Tudor Vianu” National College, Bucharest & National Institute for Research and Development in Electrical Engineering ICPE-CA Bucharest (INCDIE ICPE-CA)
 eduard.albei@gmail.com

Abstract - This paper aims to provide an explanation of the basics of manipulating three-dimensional vectors through quaternion operations and/or transformation matrices. The paper captures the practical use of this knowledge in the design of a computer-assisted pilot helmet.

Index Terms: quaternion, matrix, geometry, heads-up display, orientation, human interface

I. Mathematical Considerations

A point in space, p , can be represented in a three-dimensional Cartesian coordinate system as a triplet of values $x, y, z \in \mathbb{R}$ as follows:

$$p = x\vec{i} + y\vec{j} + z\vec{k}$$

Where \vec{i}, \vec{j} and \vec{k} are the versors of the perpendicular axes of the system, and therefore, they are unit-vectors. We deduce that the point p is also vectorial in nature. A plane or a geometric body G can in turn be represented in the coordinate system as a set of points:

$$G = \{p_1, p_2, \dots, p_n\}$$

By itself, this method of reducing the geometry of an object to a set of numerical values is of limited use. Practical scenarios include not only structures, but also processes, and the need to find a mathematical representation and, implicitly, a method of memorizing these processes is just as important. From a geometric point of view, the notion of “process” is synonymous with that of “transformation”, implying the determination of a final state from the definition of an initial state. The difficulty,

then, resides in finding a reliable mathematical model for representing basic geometric transformations – an algebra of transformations, in other words. This model is expected to satisfy the following:

1. The existence of a domain that all the basic transformations are defined for, regardless of their type
2. The existence of operators that allow for sequential and cumulative application of transformations

The usage of matrix algebra is a remarkable solution to this problem, given that for any vector \vec{p} , it can be represented as a column-matrix and, as a consequence, is compatible with matrix operations.

$$p = x\vec{i} + y\vec{j} + z\vec{k} \stackrel{\text{def}}{=} \begin{cases} \begin{bmatrix} x \\ y \\ z \\ 1 \end{bmatrix} & \text{(homogenous coordinates)} \\ \begin{bmatrix} x \\ y \\ z \end{bmatrix} & \text{(Euclidean coordinates)} \end{cases}$$

Remark: The three-dimensional vector is often written as a column-matrix containing four homogeneous coordinates. Homogeneous coordinates have the following property that relates them to the Euclidean coordinate system:

$$\forall w \in \mathbb{R} \Rightarrow \begin{bmatrix} x \\ y \\ z \end{bmatrix} = \begin{bmatrix} wx \\ wy \\ wz \\ w \end{bmatrix} = \begin{bmatrix} x \\ y \\ z \\ 1 \end{bmatrix}$$

The homogeneous coordinates representation implies that matrix operations between the vector \vec{p} and transformation matrices belonging to $M_{4 \times 4}(\mathbb{R})$ are possible.

1 The Transformation Matrix

1.1 Definition

In the context of three-dimensional geometry, transformation matrices belong to $M_{4 \times 4}(\mathbb{R})$ or $M_{3 \times 3}(\mathbb{R})$, depending on the coordinate system in which calculations are performed. The application of a transformation on a point p in order to obtain the transformed point p' is done by simply multiplying to the left with the transformation matrix A .

$$p' = A \cdot p$$

Remark: Matrices belonging to $M_{4 \times 4}(\mathbb{R})$ differ from those in $M_{3 \times 3}(\mathbb{R})$ in that they are able to represent transformations without fixed points.

Proof: We assume that p is the origin of the coordinate system, then:

$$p = \vec{0} = \begin{bmatrix} 0 \\ 0 \\ 0 \end{bmatrix} \Rightarrow$$

$$\forall A \in M_{3 \times 3}(\mathbb{R}) \quad A \cdot p = \begin{bmatrix} 0 \\ 0 \\ 0 \end{bmatrix} = p$$

Therefore, $\nexists A \in M_{3 \times 3}(\mathbb{R})$ such that $A \cdot p \neq p$ when $p = \vec{0}$.

In this case there is at least one fixed point regardless of the transformation, and that is the origin.

The rest of this document will use the notation in homogeneous coordinates, making it possible to represent the matrices of many types of transformations that do not have fixed points [1].

1.2 Types of Transformations

1.2.1 Scaling

Given the set of points $G = \{p_1, p_2, \dots, p_n\}$ that defines the geometry of an object, we are required to determine the transformation matrix A that “enlarges” the object on one or more axes:

$$\forall p \in G \Leftrightarrow p = \begin{bmatrix} x \\ y \\ z \\ 1 \end{bmatrix}$$

$$A \cdot p = \begin{bmatrix} \alpha x \\ \beta y \\ \gamma z \\ 1 \end{bmatrix} \text{ where } \alpha, \beta, \gamma \neq 1$$

We determine the general form of the transformation matrix by using the analytical method:

$$\begin{aligned} A \cdot p &= \begin{bmatrix} a_{11} & a_{12} & a_{13} & a_{14} \\ a_{21} & a_{22} & a_{23} & a_{24} \\ a_{31} & a_{32} & a_{33} & a_{34} \\ 0 & 0 & 0 & 1 \end{bmatrix} \begin{bmatrix} x \\ y \\ z \\ 1 \end{bmatrix} \\ &= \begin{bmatrix} a_{11}x + a_{12}y + a_{13}z + a_{14} \\ a_{21}x + a_{22}y + a_{23}z + a_{24} \\ a_{31}x + a_{32}y + a_{33}z + a_{34} \\ 1 \end{bmatrix} \\ &= \begin{bmatrix} \alpha x \\ \beta y \\ \gamma z \\ 1 \end{bmatrix} \end{aligned}$$

Which gives us:

$$A = \begin{bmatrix} \alpha & 0 & 0 & 0 \\ 0 & \beta & 0 & 0 \\ 0 & 0 & \gamma & 0 \\ 0 & 0 & 0 & 1 \end{bmatrix}$$

We will proceed similarly for the rest of the usual transformations.

1.2.2 Rotation

Given the set of points $G = \{p_1, p_2, \dots, p_n\}$ that defines the geometry of an object, we are required to determine three transformation matrices marked as A_{Ox} , A_{Oy} and A_{Oz} that “rotate” the object counter clockwise about the Ox , Oy and Oz axes of the coordinate system,

respectively. Let us first try to determine the general form of the transformation matrix A_{Oz} .

It is known that a rotation about the axis Oz :

1. Will not affect the z coordinate of point p .
2. Will be equivalent to a rotation around the origin, in the plane defined by the axes Ox and Oy .

Consequently, the transformation matrix will be of the form:

$$A_{Oz} \cdot p = \begin{bmatrix} a_{11}x + a_{12}y + a_{13}z + a_{14} \\ a_{21}x + a_{22}y + a_{23}z + a_{24} \\ a_{31}x + a_{32}y + a_{33}z + a_{34} \\ 1 \end{bmatrix} = \begin{bmatrix} x' \\ y' \\ z \\ 1 \end{bmatrix} \quad (1)$$

Regarding rotation in the Ox - Oy plane, the notion of “angle” is determined counter clockwise, relative to the Ox axis. It is required that we determine the relation that describes the variation of the x and y coordinates of point p following a rotation of θ_1 radians starting from an initial angle θ_0 , relative to the Ox axis. We know the following:

$$\begin{aligned} |\vec{p}| &= \sqrt{x^2 + y^2} \\ \theta_0 &= \sin^{-1} \frac{y}{|\vec{p}|} = \cos^{-1} \frac{x}{|\vec{p}|} \\ (x, y) &= (|\vec{p}| \cos \theta_0, |\vec{p}| \sin \theta_0) \end{aligned}$$

Thus:

$$\begin{aligned} x' &= |\vec{p}| \cos(\theta_0 + \theta_1) \\ &= |\vec{p}| (\cos \theta_0 \cos \theta_1 - \sin \theta_0 \sin \theta_1) \\ &= |\vec{p}| \left(\cos \left(\cos^{-1} \frac{x}{|\vec{p}|} \right) \cos \theta_1 \right. \\ &\quad \left. - \sin \left(\sin^{-1} \frac{y}{|\vec{p}|} \right) \sin \theta_1 \right) \\ &= x \cos \theta_1 + y \sin \theta_1 \end{aligned} \quad (2)$$

In the same manner, we get:

$$y' = y \cos \theta_1 + x \sin \theta_1 \quad (3)$$

Relations (1), (2) and (3) imply that:

$$\begin{aligned} A_{Oz} \cdot p &= \begin{bmatrix} x' \\ y' \\ z \\ 1 \end{bmatrix} \\ &= \begin{bmatrix} a_{11}x + a_{12}y + a_{13}z + a_{14} \\ a_{21}x + a_{22}y + a_{23}z + a_{24} \\ a_{31}x + a_{32}y + a_{33}z + a_{34} \\ 1 \end{bmatrix} \\ &= \begin{bmatrix} x \cos \theta_1 + y \sin \theta_1 \\ y \cos \theta_1 + x \sin \theta_1 \\ z \\ 1 \end{bmatrix} \end{aligned}$$

Lastly:

$$A_{Oz} = \begin{bmatrix} \cos \theta_1 & -\sin \theta_1 & 0 & 0 \\ \sin \theta_1 & \cos \theta_1 & 0 & 0 \\ 0 & 0 & 1 & 0 \\ 0 & 0 & 0 & 1 \end{bmatrix}$$

The general forms of A_{Ox} and A_{Oy} are similarly determined as:

$$\begin{aligned} A_{Ox} &= \begin{bmatrix} 1 & 0 & 0 & 0 \\ 0 & \cos \theta_1 & -\sin \theta_1 & 0 \\ 0 & \sin \theta_1 & \cos \theta_1 & 0 \\ 0 & 0 & 0 & 1 \end{bmatrix} \\ A_{Oy} &= \begin{bmatrix} \cos \theta_1 & 0 & \sin \theta_1 & 0 \\ 0 & 1 & 0 & 0 \\ -\sin \theta_1 & 0 & \cos \theta_1 & 0 \\ 0 & 0 & 0 & 1 \end{bmatrix} \end{aligned}$$

1.2.3 Translation

Given the set of points $G = \{p_1, p_2, \dots, p_n\}$ that defines the geometry of an object, we are required to determine the transformation matrix A that “moves” the object along one or more axes:

$$\begin{aligned} \forall p \in G \Leftrightarrow p &= \begin{bmatrix} x \\ y \\ z \\ 1 \end{bmatrix} \\ A \cdot p &= \begin{bmatrix} x + \alpha \\ y + \beta \\ z + \gamma \\ 1 \end{bmatrix} \text{ where } \alpha, \beta, \gamma \neq 0 \end{aligned}$$

Thus:

$$A \cdot p = \begin{bmatrix} a_{11}x + a_{12}y + a_{13}z + a_{14} \\ a_{21}x + a_{22}y + a_{23}z + a_{24} \\ a_{31}x + a_{32}y + a_{33}z + a_{34} \\ 1 \end{bmatrix} = \begin{bmatrix} x + \alpha \\ y + \beta \\ z + \gamma \\ 1 \end{bmatrix}$$

Which leads to:

$$A = \begin{bmatrix} 1 & 0 & 0 & \alpha \\ 0 & 1 & 0 & \beta \\ 0 & 0 & 1 & \gamma \\ 0 & 0 & 0 & 1 \end{bmatrix}$$

Remark: Since the translation transformation has no fixed points, it can only be performed using a $A \in M_{4 \times 4}(\mathbb{R})$ matrix.

Proof: For such a transformation to exist, it is necessary that:

$$\alpha, \beta, \gamma \neq 0 \tag{4}$$

We assume that such a fixed point exists:

$$A \cdot p = p \Leftrightarrow \begin{bmatrix} x + \alpha \\ y + \beta \\ z + \gamma \\ 1 \end{bmatrix} = \begin{bmatrix} x \\ y \\ z \\ 1 \end{bmatrix} \Leftrightarrow (\alpha, \beta, \gamma) = (0,0,0) \tag{5}$$

Relations (4) and (5) result in a contradiction, therefore, our assumption can only be false.

1.2.5 Perspective Projection

An intricate but remarkably useful transformation is the perspective projection of a volume of space on a plane. This mathematical operation is the basis of the process by which a computer can use a two-dimensional screen to display the image of a three-dimensional geometric body stored in memory [2]. The perspective of the projection is defined by two known planes, α and β , aligned

concentrically and perpendicular to the Oz axis according to the example in Figure 1:

Figure 1: Perspective Frustum

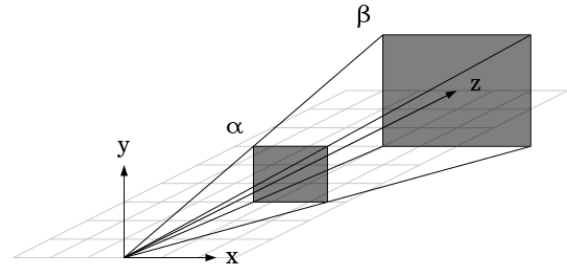
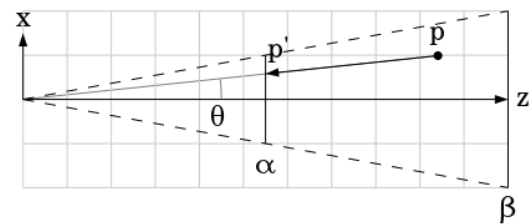


Figure 2: Cross-Section of the Frustum on the $Ox-Oz$ Plane



Given the set of points $G = \{p_1, p_2, \dots, p_n\}$ that defines the geometry of an object, we are required to determine the transformation matrix A that “projects” the object on the α plane, thus reducing it to a set of bidimensional points.

$$A \cdot p = \begin{bmatrix} a_{11}x + a_{12}y + a_{13}z + a_{14} \\ a_{21}x + a_{22}y + a_{23}z + a_{24} \\ a_{31}x + a_{32}y + a_{33}z + a_{34} \\ 1 \end{bmatrix} = \begin{bmatrix} x' \\ y' \\ z_\alpha \\ 1 \end{bmatrix} \tag{6}$$

Where z_α is a known constant, characteristic to plane α .

An example of this operation, limited to two dimensions, can be seen in Figure 2. We will determine the transformation matrix using this example.

We know the following:

$$p = (z, x)$$

$$p' = (z_\alpha, x')$$

$$\widehat{z\mathcal{O}p} = \widehat{z\mathcal{O}p'} = \theta \Leftrightarrow$$

$$\tan \widehat{z\mathcal{O}p} = \tan \widehat{z\mathcal{O}p'} \Leftrightarrow$$

$$\frac{x}{z} = \frac{x'}{z_\alpha}$$

Therefore:

$$x' = x \frac{z_\alpha}{z} \tag{7}$$

Similarly:

$$y' = y \frac{z_\alpha}{z} \tag{8}$$

Relations (6), (7) and (8) imply:

$$\begin{bmatrix} a_{11}x + a_{12}y + a_{13}z + a_{14} \\ a_{21}x + a_{22}y + a_{23}z + a_{24} \\ a_{31}x + a_{32}y + a_{33}z + a_{34} \\ 1 \end{bmatrix} = \begin{bmatrix} x \frac{z_\alpha}{z} \\ y \frac{z_\alpha}{z} \\ z_\alpha \\ 1 \end{bmatrix}$$

However, we notice that:

$$\exists (a_{11}, a_{12}, a_{13}, a_{14}) \in \mathbb{R} \text{ s. t.}$$

$$a_{11}x + a_{12}y + a_{13}z + a_{14} = x \frac{z_\alpha}{z}$$

$$\forall x, y, z \in \mathbb{R}$$

This suggests that the matrix A cannot be written as above, this problem is solved by the fundamental property of homogeneous coordinates [3]:

$$\begin{bmatrix} x \\ y \\ z \\ 1 \end{bmatrix} = \begin{bmatrix} wx \\ wy \\ wz \\ w \end{bmatrix} \Leftrightarrow p' = \begin{bmatrix} x \frac{z_\alpha}{z} \\ y \frac{z_\alpha}{z} \\ z_\alpha \\ 1 \end{bmatrix} = \begin{bmatrix} xz_\alpha \\ yz_\alpha \\ zz_\alpha \\ z \end{bmatrix}$$

Consequently, the general form of A can be determined using the analytical method:

$$A \cdot p = \begin{bmatrix} a_{11} & a_{12} & a_{13} & a_{14} \\ a_{21} & a_{22} & a_{23} & a_{24} \\ a_{31} & a_{32} & a_{33} & a_{34} \\ a_{41} & a_{42} & a_{43} & a_{44} \end{bmatrix} \begin{bmatrix} x \\ y \\ z \\ 1 \end{bmatrix}$$

$$= \begin{bmatrix} xz_\alpha \\ yz_\alpha \\ zz_\alpha \\ z \end{bmatrix} \Leftrightarrow$$

$$A = \begin{bmatrix} z_\alpha & 0 & 0 & 0 \\ 0 & z_\alpha & 0 & 0 \\ 0 & 0 & z_\alpha & 0 \\ 0 & 0 & 1 & 0 \end{bmatrix}$$

1.3 Usage

Given the transformation matrices $A, B, C \in M_{4 \times 4}(\mathbb{R})$ and point p , because matrix multiplication is associative, the following is true:

$$C \cdot (B \cdot (A \cdot p)) = (C \cdot B \cdot A) \cdot p$$

Axiom: Applying a transformation defined by a product of transformation matrices is equivalent to the right-to-left successive application of all transformations of the matrices involved in the product [4].

2 The Quaternion

2.1 Definition

The following is the set of Hamiltonian numbers, also known as quaternions:

$$\mathbb{H} = \{a + bi + cj + dk \mid a, b, c, d \in \mathbb{R}\}$$

where $i^2 = j^2 = k^2 = ijk = -1$

In other words, a quaternion is a four-dimensional number. Given the fundamental property of the imaginary numbers i, j and k , the following tabular description of all possible products can be derived:

\cdot	1	i	j	k
1	1	i	j	k
i	i	-1	k	$-j$
j	j	$-k$	-1	i
k	k	j	$-i$	-1

Using the table above as a reference, quaternion calculations are performed according to the same laws of operation with real numbers.

By definition, the real and imaginary components of a quaternion q are:

$$\begin{aligned} \operatorname{Re}(q) &= a \\ \operatorname{Im}(q) &= bi + cj + dk \end{aligned}$$

The conjugate of a quaternion q is written as q^* and satisfies the following property:

$$\begin{aligned} \forall q &= a + bi + cj + dk \\ \exists q^* &= a - bi - cj - dk \end{aligned}$$

Which implies:

$$\frac{q + q^*}{2} = \operatorname{Re}(q)$$

The conjugate can be used for calculating the norm $|q|$ of a quaternion:

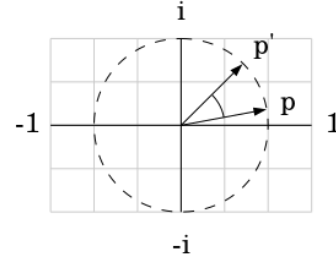
$$|q| = \sqrt{qq^*} = \sqrt{a^2 + b^2 + c^2 + d^2}$$

Quaternions with norm $|q| = 1$, also known as unit-vectors, are particularly useful, they can be used to define directions in three-dimensional space.

2.2 Usage

To demonstrate the immediate utility of quaternions, the following analogy of one of the properties of complex numbers is proposed in Figure 3.

Figure 3: Rotation of Complex Numbers Through Multiplication



Axiom: Let:

$$p, q \in \mathbb{C} \text{ s. t. } |q| = 1; pq = p'$$

Then:

$$\begin{aligned} |p'| &= |p| \\ \theta_{p'} &= \theta_p + \theta_q \Leftrightarrow \\ \tan^{-1} \frac{\operatorname{Im}(p')}{\operatorname{Re}(p')} &= \\ &= \tan^{-1} \frac{\operatorname{Im}(p)}{\operatorname{Re}(p)} + \tan^{-1} \frac{\operatorname{Im}(q)}{\operatorname{Re}(q)} \end{aligned}$$

Where θ_z is the angle of the complex number z .

A complex number can be “rotated” in the plane of complex numbers by multiplying by another complex number of unitary magnitude. In general, when two complex numbers are multiplied, their magnitudes multiply and their angles add up.

Proof: Let $p, q \in \mathbb{C}$ where $(p, q) = (a + bi, c + di)$ then:

$$\begin{aligned} \theta_p &= \tan^{-1} \frac{b}{a} \\ \theta_q &= \tan^{-1} \frac{d}{c} \\ |p| &= \sqrt{a^2 + b^2} \\ |q| &= \sqrt{c^2 + d^2} \\ pq &= (a + bi)(c + di) \\ &= ac - bd + i(ad + bc) \end{aligned}$$

Consequently:

$$\begin{aligned}
 |pq| &= \sqrt{(ac - bd)^2 + (ad + bc)^2} \\
 &= \sqrt{(ac)^2 - 2abcd + (bd)^2 + (ad)^2 + 2abcd + (bc)^2}
 \end{aligned}
 \tag{9}$$

$$\begin{aligned}
 |p||q| &= \sqrt{(a^2 + b^2)(c^2 + d^2)} \\
 &= \sqrt{(ac)^2 + (bd)^2 + (ad)^2 + (bc)^2}
 \end{aligned}
 \tag{10}$$

$$\theta_{pq} = \tan^{-1} \frac{ad + bc}{ac - bd}
 \tag{11}$$

$$\begin{aligned}
 \theta_p + \theta_q &= \tan^{-1} \frac{b}{a} + \tan^{-1} \frac{d}{c} \\
 &= \tan^{-1} \frac{\frac{b}{a} + \frac{d}{c}}{1 - \frac{bd}{ac}} \\
 &= \tan^{-1} \frac{ad + bc}{ac - bd}
 \end{aligned}
 \tag{12}$$

Relations (9) and (10) imply $|pq| = |p||q|$, while (11) and (12) imply $\theta_{pq} = \theta_p + \theta_q$, QED.

Quaternions behave similarly, but on a different level. The following relationship captures this aspect:

$$\mathbb{R} \subset \mathbb{C} \subset \mathbb{H}$$

Similar to how the entire axis of real numbers is included in \mathbb{C} , the entire domain of three-dimensional vectors is included in \mathbb{H} . A purely imaginary quaternion is nothing but such a vector. Given the set of points $G = \{p_1, p_2, \dots, p_n\}$ that defines the geometry of an object, then:

$$\forall p \in G \quad p = \begin{bmatrix} x \\ y \\ z \end{bmatrix} = xi + yj + zk \in \mathbb{H}$$

Moreover, the fundamental property of the imaginary numbers i, j and k implies that the rotation of a three-dimensional point p by θ radians about an axis defined by the three-dimensional unit vector α with the purpose of obtaining the

transformed point p' is equivalent to the following operation [5]:

$$p' = qpq^* \quad | \quad q = \cos \frac{\theta}{2} + \alpha \sin \frac{\theta}{2}$$

This method of rotating three-dimensional points is more efficient and less prone to error than the use of transformation matrices. Suppose we intend to perform the same rotation around some axis α using only transformation matrices:

Because we only know the general forms of matrices for the rotational transformations around the three axes Ox , Oy and Oz , we are required to determine what product of rotations around the three known axes is equivalent to the desired rotation of θ radians about the axis α :

$$p' = (A_{Ox} \cdot A_{Oy} \cdot A_{Oz})p$$

Therefore, two problems arise:

1. Determining the three transformation matrices can prove difficult
2. Once the matrices have been determined, the sequence of their application must also be memorized because the multiplication of matrices is not commutative:

$$(A_{Ox} \cdot A_{Oy} \cdot A_{Oz})p \neq (A_{Ox} \cdot A_{Oz} \cdot A_{Oy})p$$

As such, it is recommended to establish a convention regarding the order in which rotational transformations are applied.

II. Technical Implementation

3 Schematic Description of the System

The system in question is a portable computing platform, focused on (but not limited to) the generation and manipulation of a video stream projected on the retina. The main use case of this system is of a computer-assisted pilot helmet. The working principle involves the usage of computational resources and an integrated video camera assembly to replace the pilot's eyesight with a pre-processed video stream. The following are the system's requirements:

1. Possibility for the wearer to use the video stream in a way that is as faithful as possible to normal eyesight
2. Introduction of an advantage over normal eyesight through specific functions of the camera assembly, functions such as: infrared spectrum view, self-illumination, image magnification, etc.
3. Integration of a wide array of communication interfaces to external equipment used by the pilot
4. Possibility of full manipulation of the video stream for purposes such as: display of pilot data in the field of view, display of text-based telecommunications, selective highlighting of silhouettes, recognition and marking of objects in the field of view, etc.
5. Use of the helmet's sensor assembly in determining the spatial orientation of the pilot for rendering indicators such as: artificial horizon, digital compass, elevation measurements, etc.
6. Connection to the wide area network (WAN)
7. Ability to run for at least 2 hours in the absence of a power source

Figure 4: Software Components

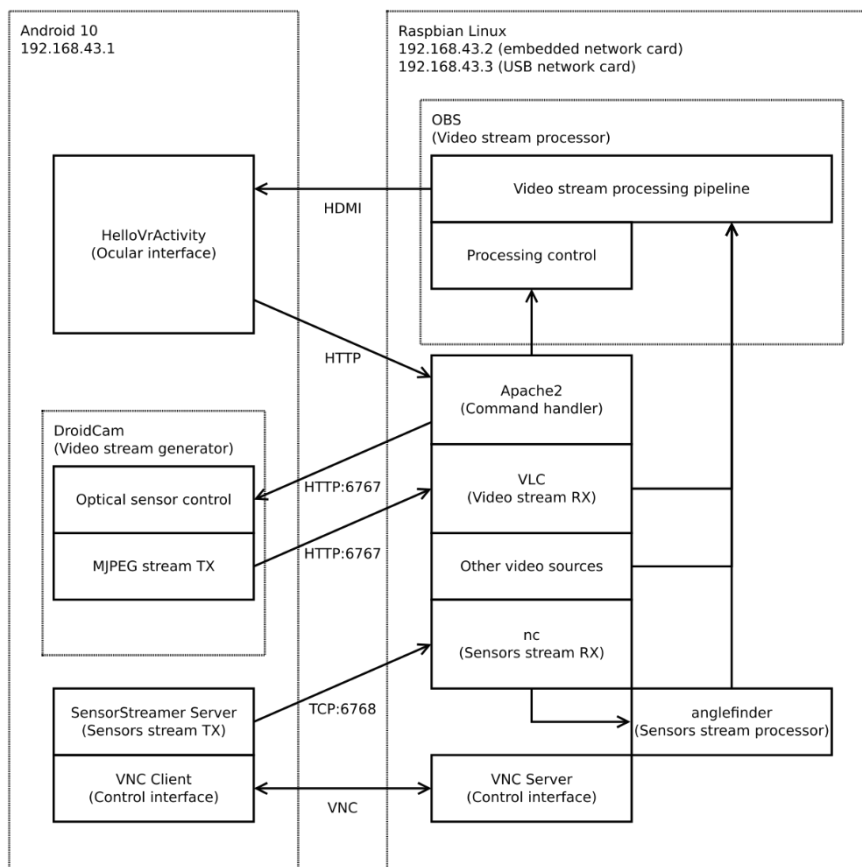
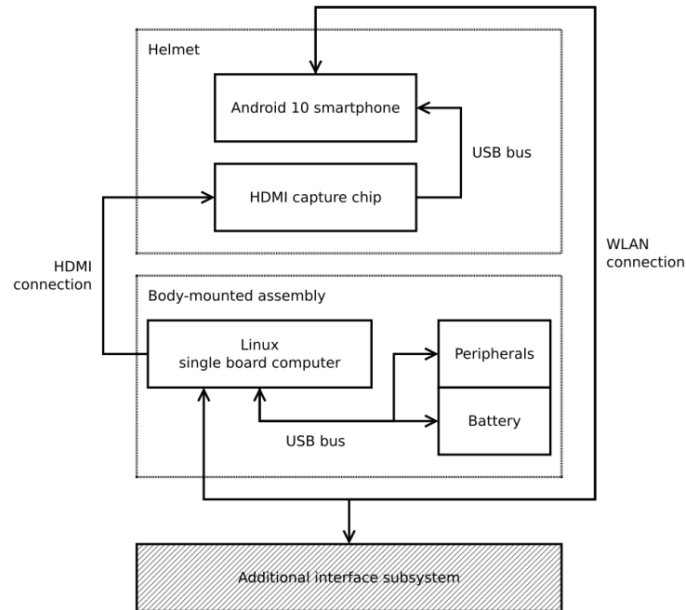


Figure 5: Hardware Components



4 Usage of Mathematical Concepts

4.1 The Transformation Matrix

Once the video stream is generated by the optical sensor assembly and pre-processed by the computer, it must be projected through the helmet's lens to the

pilot's retina. This is done by rendering a virtual screen that displays this stream in front of the pilot. Figure 6 contains a sample of the code that drives the graphics chip to multiply a transformation matrix with each of the points that describe the geometry of the aforementioned virtual screen.

Figure 6: GLSL Source Code

```
uniform mat4 VP;
attribute vec2 vPos;
attribute vec2 vTex;
varying vec2 v_UV;
void main()
{
    v_UV = vTex;
    gl_Position = VP * vec4(vPos.x, vPos.y, -1.0, 1.0);
}
```

A matrix belonging to $M_{4 \times 4}(\mathbb{R})$ is stored inside the variable “VP”. The function “vec4(x, y, z, w)” only uses the necessary coordinates of the vector “vPos” for deducing the point on which the transformation described by the contents of “VP” will be applied. The result of left multiplying the point with the transformation matrix is stored in “gl_Position”, this value represents the transformed point.

4.2 The Quaternion

Each reading from the helmet's orientation sensors consists of three of the coordinates of a unit-quaternion that describes the pilot's spatial orientation at the time of reading. For all unit-quaternions the following relation is true:

$$|q| = \sqrt{a^2 + b^2 + c^2 + d^2} = 1$$

Consequently, the fourth coordinate of the quaternion must not be transmitted and can be deduced. Figure 7

contains a sample of the code used by the computer to render the artificial horizon indicators over the pilot's field of view.

Relevant comments have been inserted into the code.

Figure 7: C++ Source Code

```
//STEP 1: Read essential unit-quaternion components and
initialise heading vectors
for(short i=0; i<3; i++)
{
    cin >> quatraw[i];
    fwdupright[i].set(initraw+i*3);
}

//STEP 2: Deduce unessential component
quatraw[3] = sqrt(1 - quatraw[0]*quatraw[0] -
quatraw[1]*quatraw[1] - quatraw[2]*quatraw[2]);

//STEP 3: Assemble quaternion
quat.set(quatraw[0], quatraw[1], quatraw[2], quatraw[3]);

//STEP 4: Apply quaternion rotation to heading vectors and
optionally plot them or just print results
for(short i=0; i<3; i++)
{
    fwdupright[i] = quat * fwdupright[i];
    *(xcoords[i]) = (fwdupright[i].getData())[0];
    *(ycoords[i]) = (fwdupright[i].getData())[1];
    *(zcoords[i]) = (fwdupright[i].getData())[2];
}
```

III. Final Results

Figure 8 contains the QR code of the **hrihelm.iso** SD card image. The system contains a large number of changes to the Raspbian Linux distribution. For this reason, the software is distributed as an entire system image, instead of an installable package. An SD card with a capacity of at least 32GB is required for full image transcription. Transcription on the system's SD card #0 can be done through the corresponding command sequence.

Figure 8: QR Code of the SD Card Image



```
unxz hrihelm.iso.xz;
dd if=hrihelm.iso \
of=/dev/mmcblk0
```

Notice: The password of the main user of the system is: 91142067

Notice: In its current state, the system automatically connects to the hotspot network of the author's smartphone. Consequently, when another smartphone is used as part of the helmet, the system must be configured accordingly.

Figure 9: QR Code of the Android Retinal Interface App



Figure 10: QR Code of the Demo Footage



Figure 9 contains the QR code of the Android Studio project that implements the retinal interface of the system. Read Figure 4 for details on how the interface is integrated into the system.

The system start-up procedure, followed by the use of certain functions is exemplified in the footage identified by the QR code in Figure 10.

5 Testing

Figure 11: Helmet and Body-Mounted Assembly



Figure 12: Helmet's Profile, HDMI Capture Chip Visible



Figure 13: Looking at a Mirror



Figure 14: Tracking a Small-Sized Animal



Figure 15: Selective Highlighting of Silhouettes



IV. References

- [1] N. Pollard, “15-462: Computer Graphics: Chapter 4, Transformations”, spring 2004
<http://graphics.cs.cmu.edu/nsp/course/15-462/Spring04/slides/04-transform.pdf>
- [2] J. Santell, “Model View Projection”, 14 April 2019
<https://jsantell.com/model-view-projection/>
- [3] T. Dalling, “Explaining Homogeneous Coordinates & Projective Geometry”, 24 February 2014
<https://www.tomdalling.com/blog/modern-opengl/explaining-homogenous-coordinates-and-projective-geometry/>
- [4] H. Wang, “CSE 5542: Real-Time Rendering: Composing Transformations”, spring 2013
http://web.cse.ohio-state.edu/~wang.3602/courses/cse5542-2013-spring/6-Transformation_II.pdf
- [5] A. Bennett, V. Kindratenko, “Quaternions and Their Properties”, 29 August 2000
<https://users.ncsa.illinois.edu/kindr/emtc/quaternions/>

V. Biography

Albei Victor-Eduard



Born 31 December 2002

High school student in the XIIth grade at “Tudor Vianu” National College of Computer Science

Telecommunications engineering enthusiast.

Former online broadcasting station technician

Description of the Fourier Transform and the Development of an Audio-Based Replacement for the RS-232 Standard

Albei Victor-Eduard

“Tudor Vianu” National College, Bucharest & National Institute for Research and Development in Electrical Engineering ICPE-CA Bucharest (INCDIE ICPE-CA)
eduard.albei@gmail.com

Abstract - This paper contains a series of demonstrations of the mathematical principles underlying analog signal processing. It offers a definition of the Fourier transform, its application on discrete values and its interpretation in the form of an algorithm of minimal complexity. The paper exemplifies the above concepts in designing a protocol for data transfer through audio signals.

Index Terms: spectrum analysis, communications protocol, signal processing, analog, computer terminal, audio

I. Mathematical Definition

An analog signal can be defined as a value that belongs to an interval of real

$$A = \{f(t) \mid f: \mathbb{R} \rightarrow (a, b); f(t) = f(t + k); a, b, k \in \mathbb{R}\}$$

The function $f(t) = \cos(t)$ is considered to be the simplest function belonging to the set A because, according to the Fourier theorem [1], any periodic function can be written as a sum of $n \in \mathbb{N}$ cosine functions of different amplitudes, frequencies and

$$\forall f \in A, \quad \exists (a_k, \theta_k) \in \mathbb{R} \times \mathbb{R}, \nu_k \in \mathbb{R} \mid k \in \{0, 1, \dots, n-1\} \text{ s. t.}$$

$$f(t) = \sum_{k=0}^{n-1} a_k \cos(2\pi\nu_k t + \theta_k)$$

$$E = \{g(t) = a \cos(2\pi\nu t + \theta) \mid g: \mathbb{R} \rightarrow [-1, 1]; a, \nu, \theta \in \mathbb{R}\}$$

1 The Fourier Transform

Given the analog signal $f \in A$ which contains the basic analog signal $g \in E$, where $\nu_g \in \mathbb{R}^+$ is the only known parameter of signal g , we are required to determine its other defining parameters (a_g, θ_g) .

numbers. If there is a relation between the signal's value and another parameter, it can be modelled as a mathematical function. The set of time-dependent analog signals can be defined as follows:

$$A = \{f(t) \mid f: \mathbb{R} \rightarrow \mathbb{R}\}$$

For practical reasons, analog signals take on values that belong to finite intervals, a consequence of which is that periodicity is a common feature of all signals defined on infinite intervals. Therefore, the following would be a more precise definition:

phase shifts, as shown in (1). Throughout this paper, all terms of the sum (1) will be referred to as “basic analog signals”. The set of basic analog signals takes on the form (2).

The solution to this problem can be determined using the Fourier transform of the signal f for the frequency ν_g , marked as $\hat{f}(\nu_g)$. In order to understand the mathematical principles behind this transform, we will use the alternative definition (8) of basic analog signals.

1.1 Euler's Formula

The following identity is given:

$$e^{ix} = \cos(x) + i \sin(x) \quad \forall x \in \mathbb{R} \quad (3)$$

Proof:

$$\begin{aligned} e^{ix} &= \cos(x) + i \sin(x) \Leftrightarrow \\ ix &= \ln(\cos(x) + i \sin(x)) \end{aligned} \quad (4)$$

Two functions are considered, $f, g: \mathbb{R} \rightarrow \mathbb{C}$, representing the left-hand side and the right-hand side of (4):

$$f(x) = ix; g(x) = \ln(\cos(x) + i \sin(x))$$

Two functions are equal if they differ by a constant value and that constant is null:

$$f(x) = g(x) \Leftrightarrow \begin{cases} f(x) = g(x) + k \\ k = 0 \end{cases} \quad (5)$$

$$\begin{aligned} f'(x) = g'(x) &\Leftrightarrow \frac{i \cos(x) - \sin(x)}{\cos(x) + i \sin(x)} = i \\ &\Leftrightarrow \frac{\cos(x) + i \sin(x)}{\cos(x) + i \sin(x)} = 1 \end{aligned} \quad (6)$$

$$f(0) = g(0) \quad (7)$$

Relations (5), (6) and (7) imply (3), QED.

1.2 The Representation of an Analog Signal

Given (2), we deduce that the basic analog signal can be defined as:

$$\cos(x) = \frac{[\cos(x) + i \sin(x)] + [\cos(x) - i \sin(x)]}{2} = \frac{e^{ix} + e^{-ix}}{2} \quad (8)$$

Let (1) and (8) be known, then:

$$\begin{aligned} \forall g \in E \\ g(t) &= \frac{a}{2} (e^{i2\pi vt + i\theta} + e^{-i2\pi vt - i\theta}) \end{aligned} \quad (9)$$

$$\begin{aligned} \forall f \in A \\ f(t) &= \sum_{k=0}^{n-1} g_k(t) \\ &= \frac{1}{2} \sum_{k=0}^{n-1} a_k (e^{i2\pi v_k t + i\theta_k} + e^{-i2\pi v_k t - i\theta_k}) \end{aligned} \quad (10)$$

1.3 Operations on Analog Signals

Given the signal $f \in A$ and identity (10), the following are true:

$$\begin{aligned} f(t)e^{-i2\pi vt} &= \left[\frac{1}{2} \sum_{k=0}^{n-1} a_k (e^{i2\pi v_k t + i\theta_k} + e^{-i2\pi v_k t - i\theta_k}) \right] e^{-i2\pi vt} \\ &= \frac{1}{2} \sum_{k=0}^{n-1} a_k (e^{i2\pi v_k t + i\theta_k} \cdot e^{-i2\pi vt} + e^{-i2\pi v_k t - i\theta_k} \cdot e^{-i2\pi vt}) \\ &= \frac{1}{2} \sum_{k=0}^{n-1} a_k (e^{i2\pi(v_k - v)t + i\theta_k} + e^{-i2\pi(v_k + v)t - i\theta_k}) \end{aligned} \quad (11)$$

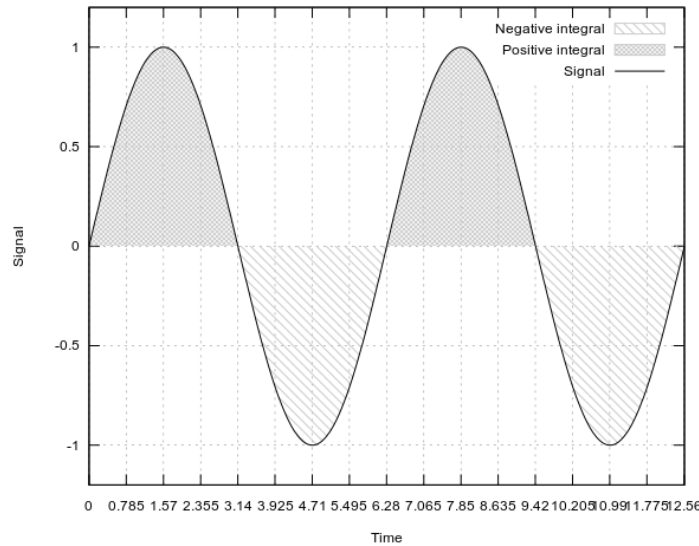
At the same time:

$$e^{i2\pi vt+i\theta} = \begin{cases} \cos(2\pi vt + \theta) + i \sin(2\pi vt + \theta) & v \neq 0 \\ \cos(\theta) + i \sin(\theta) & v = 0 \end{cases} \tag{12}$$

$$\int_{-\infty}^{\infty} \cos(t) dt = \int_{-\infty}^{\infty} \sin(t) dt = 0 \tag{13}$$

See Figure 1 for details regarding (13).

Figure 1: Integration of a Sine Wave Over an Infinite Interval



Remark: The periodicity of the function and the integration on the infinite interval guarantee that, for $k \in \mathbb{R}$, the following are true:

$$\begin{aligned} \forall I &= \int_{2k\pi}^{2(k+1)\pi} \cos(x) dx, \\ \exists I' &= \int_{2(k+1)\pi}^{2(k+2)\pi} \cos(x) dx \text{ s. t.} \\ I + I' &= 0 \end{aligned} \tag{14}$$

Relations (12) and (13) imply that:

$$\begin{aligned} \int_{-\infty}^{\infty} e^{i2\pi vt+i\theta} dt &= \\ &= \begin{cases} 0 & v \neq 0 \\ (\cos \theta + i \sin \theta) \cdot \infty & v = 0 \end{cases} \end{aligned} \tag{15}$$

Therefore, by integrating relation (11), we get:

$$\begin{aligned} \int_{-\infty}^{\infty} f(t)e^{-i2\pi vt} dt &= \int_{-\infty}^{\infty} \frac{1}{2} \sum_{k=0}^{n-1} a_k (e^{i2\pi(v_k-v)t+i\theta_k} + e^{-i2\pi(v_k+v)t-i\theta_k}) \\ &= \frac{1}{2} \sum_{k=0}^{n-1} a_k \left(\int_{-\infty}^{\infty} e^{i2\pi(v_k-v)t+i\theta_k} dt + \int_{-\infty}^{\infty} e^{-i2\pi(v_k+v)t-i\theta_k} dt \right) \end{aligned}$$

Where:

$$\begin{aligned} &v, v_k \in \mathbb{R}^+, k \in \{0, 1, \dots, n-1\} \text{ s. t.} \\ &\begin{cases} v_k - v = 0 & v_k = v \\ v_k + v \neq 0 & \forall v_k, v \in \mathbb{R}^+ \end{cases} \end{aligned}$$

Consequently, the function resulting from the integration is one of the forms of the Fourier transform:

$$\hat{f}(v) = \int_{-\infty}^{\infty} f(t)e^{-i2\pi vt} dt = \begin{cases} 0 & \nexists k \in \{0,1, \dots, n-1\} \text{ s.t. } v_k = v \\ \frac{a_k}{2} (\cos \theta_k + i \sin \theta_k) \cdot \infty & \exists k \in \{0,1, \dots, n-1\} \text{ s.t. } v_k = v \end{cases} \quad (16)$$

This function takes on the value ∞ only in cases where the test frequency, v , is equal to any of the frequencies of the basic analog signals that are part of the signal f .

2 The Discrete Fourier Transform (DFT)

Form (16) of the Fourier transform can be restricted to a finite integration interval (a, b) with $a, b \in \mathbb{R}$ and rewritten as a Riemann sum as follows:

$$\hat{f}(v) = \int_a^b f(t)e^{-i2\pi vt} dt = \lim_{n \rightarrow \infty} \sum_{k=0}^{n-1} f\left(a + k \frac{b-a}{n}\right) e^{-i2\pi v\left(a + k \frac{b-a}{n}\right)} \frac{b-a}{n}$$

Given the periodicity of the signal, integrating on the time interval $(0, \lambda)$, $\lambda \in \mathbb{R}$, will be considered, in order to simplify the expression:

$$\begin{aligned} \hat{f}(v) &= \int_0^\lambda f(t)e^{-i2\pi vt} dt \\ &= \lim_{n \rightarrow \infty} \sum_{k=0}^{n-1} f\left(\frac{k\lambda}{n}\right) e^{-i2\pi v \frac{k\lambda}{n}} \frac{\lambda}{n} \end{aligned} \quad (17)$$

Remark: Unlike (13), the integration of a basic analog signal over a finite interval introduces errors, as (14) does not apply to finite intervals:

$$\int_0^\lambda \cos(t) dt \in [-1,1]$$

Under practical circumstances, the signal f is represented by the array of

$$\hat{f}_d(v) = \begin{cases} \Delta & \nexists k \in \{0,1, \dots, n-1\} \text{ s.t. } v_k = v \\ \frac{a_k}{2} (\cos \theta_k + i \sin \theta_k) \lambda & \exists k \in \{0,1, \dots, n-1\} \text{ s.t. } v_k = v \end{cases}$$

By normalizing this result, we get:

$$\hat{f}_d(v) = \frac{2}{\lambda R} \sum_{k=0}^{\lambda R-1} f_k e^{-i2\pi v \frac{k}{R}} = \begin{cases} \frac{2\Delta}{\lambda} & \nexists k \in \{0,1, \dots, n-1\} \text{ s.t. } v_k = v \\ a_k (\cos \theta_k + i \sin \theta_k) & \exists k \in \{0,1, \dots, n-1\} \text{ s.t. } v_k = v \end{cases} \quad (18)$$

measurements $(f_n)_{n \in \mathbb{N}}$ that have been performed on it. Measuring a signal involves the usage of a sampling rate, $R \in \mathbb{N}^*$, expressed in measurements per second:

$$f_n = f\left(\frac{n}{R}\right)$$

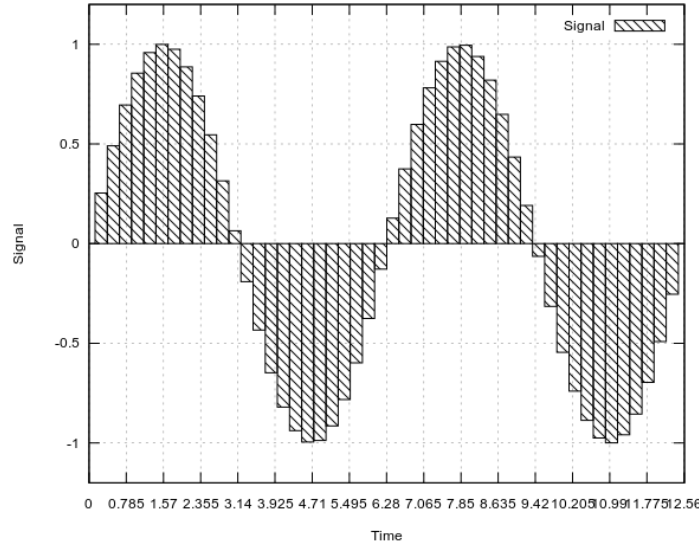
By substituting the analog signal f with the array of measurements $(f_n)_{n \in \mathbb{N}}$ in relation (17), while $\lambda \in \mathbb{R} \mid \lambda R \in \mathbb{N}^*$, the following expression is obtained, a form of the discrete Fourier transform:

$$\begin{aligned} \hat{f}_d(v) &= \sum_{k=0}^{\lambda R-1} f\left(\frac{k\lambda}{\lambda R}\right) e^{-i2\pi v \frac{k\lambda}{\lambda R}} \frac{\lambda}{\lambda R} \\ &= \frac{1}{R} \sum_{k=0}^{\lambda R-1} f_k e^{-i2\pi v \frac{k}{R}} \end{aligned}$$

Therefore:

$$\begin{cases} \Delta & \nexists k \in \{0,1, \dots, n-1\} \text{ s.t. } v_k = v \\ a_k (\cos \theta_k + i \sin \theta_k) & \exists k \in \{0,1, \dots, n-1\} \text{ s.t. } v_k = v \end{cases}$$

Figure 2: Usage of an Approximate Sum as a Practical Alternative to Integration



By comparing the Fourier transform, $\hat{f}(v)$ presented in (16), with its discrete form, $\hat{f}_d(v)$ in (18), we note that rewriting the integral as an approximate sum on the finite interval $(0, \lambda)$ solves the problem of infinite values, instead introducing the error Δ , negligible when $\lambda \rightarrow \infty$.

This function takes on values that satisfy the requirement stated at the beginning of this paper. Given the analog signal $f \in A$ which contains the basic analog signal $g \in E$, where $v_g \in \mathbb{R}^+$ is the only known parameter of signal g , the following are true:

$$a_g = |\hat{f}_d(v_g)|$$

$$\theta_g = \sin^{-1} \left(\frac{\text{Im} \hat{f}_d(v_g)}{|\hat{f}_d(v_g)|} \right)$$

Where $\text{Im}(z)$ is the imaginary component of the complex number z .

Remark: Sampling a signal involves the existence of a frequency limit [2] for which the discrete Fourier transform is defined:

$$\hat{f}_d(v): \left[0, \frac{R}{2} \right] \rightarrow \mathbb{C} \tag{19}$$

2.1 The Polynomial Form

The following is the general form of a polynomial of degree n with coefficients $a_{0,1,\dots,n}$:

$$P(x) = \sum_{k=0}^n a_k x^k$$

Therefore, evaluating the discrete Fourier transform of signal f , for the frequency v , can be defined as a polynomial evaluation problem:

$$\begin{aligned} \hat{f}_d(v) = P(x) &\Leftrightarrow \\ \frac{2}{\lambda R} \sum_{k=0}^{\lambda R - 1} f_k e^{-i2\pi v \frac{k}{R}} &= \sum_{k=0}^n a_k x^k \Leftrightarrow \\ &\Leftrightarrow \begin{cases} n = \lambda R - 1 \\ a_k = \frac{2f_k}{\lambda R} \\ x = e^{-i2\pi v \frac{1}{R}} \end{cases} \end{aligned} \tag{20}$$

The complexity of evaluating a polynomial is $O(n)$.

2.2 The Matrix Form

Identity (20) implies that the discrete Fourier transform of the signal f ,

$$\begin{bmatrix} \widehat{f}_d(v_0) \\ \widehat{f}_d(v_1) \\ \widehat{f}_d(v_2) \\ \vdots \\ \widehat{f}_d(v_{n-1}) \end{bmatrix} = \frac{2}{n} \begin{bmatrix} e^{-i2\pi v_0 \frac{0}{R}} & e^{-i2\pi v_0 \frac{1}{R}} & e^{-i2\pi v_0 \frac{2}{R}} & \dots & e^{-i2\pi v_0 \frac{n-1}{R}} \\ e^{-i2\pi v_1 \frac{0}{R}} & e^{-i2\pi v_1 \frac{1}{R}} & e^{-i2\pi v_1 \frac{2}{R}} & \dots & e^{-i2\pi v_1 \frac{n-1}{R}} \\ e^{-i2\pi v_2 \frac{0}{R}} & e^{-i2\pi v_2 \frac{1}{R}} & e^{-i2\pi v_2 \frac{2}{R}} & \dots & e^{-i2\pi v_2 \frac{n-1}{R}} \\ \vdots & \vdots & \vdots & \ddots & \vdots \\ e^{-i2\pi v_{n-1} \frac{0}{R}} & e^{-i2\pi v_{n-1} \frac{1}{R}} & e^{-i2\pi v_{n-1} \frac{2}{R}} & \dots & e^{-i2\pi v_{n-1} \frac{n-1}{R}} \end{bmatrix} \begin{bmatrix} f_0 \\ f_1 \\ f_2 \\ \vdots \\ f_{n-1} \end{bmatrix} \quad (21)$$

Remark: For arbitrarily chosen values of $v_k, \forall k \in \{0, 1, \dots, n-1\}$, the product evaluation has a complexity of $O(n^2)$.

3 The Fast Fourier Transform (FFT)

Certain properties of $v_k, \forall k \in \{0, 1, \dots, n-1\}$, chosen in relation (21) can reduce the complexity of the product evaluation to $O(n \log_2 n)$. For this purpose, roots of unity will be used.

3.1 Properties of the Roots of Unity

The set of n -th roots of unity is defined as follows:

$$\begin{aligned} R_n &= \{z \in \mathbb{C} \mid z^n = 1; n \in \mathbb{Z}\} \\ &= \{z \in \mathbb{C} \mid z^n = e^{i2\pi}; n \in \mathbb{Z}\} \end{aligned} \quad (22)$$

Relations (3), (22) and the periodicity of trigonometric functions imply that:

$$\begin{aligned} R_n &= \{z \in \mathbb{C} \mid z^n = e^{i2\pi k}; k, n \in \mathbb{Z}\} \\ &= \left\{z \in \mathbb{C} \mid z = e^{i2\pi \frac{k}{n}}; k, n \in \mathbb{Z}\right\} \\ &= \left\{e^{i2\pi \frac{k}{n}} \mid k, n \in \mathbb{Z}\right\} \end{aligned}$$

For $n = 2^m \forall m \in \mathbb{N}^*$, (23) and (24) are true:

$$\begin{aligned} \forall x \in R_n \exists x' \in R_n \text{ s. t.} \\ x = -x' \Leftrightarrow x^2 = x'^2 \end{aligned} \quad (23)$$

for $n = \lambda R$ frequencies, can be defined as the product of a square matrix and a column vector, as follows:

Proof:

$$\begin{aligned} -e^{i2\pi \frac{k}{n}} &= -\cos\left(2\pi \frac{k}{n}\right) + i \sin\left(2\pi \frac{k}{n}\right) \\ &= \cos\left(2\pi \frac{k}{n} + \pi\right) + i \sin\left(2\pi \frac{k}{n} + \pi\right) \\ &= \cos\left(2\pi \frac{k + \frac{n}{2}}{n}\right) + i \sin\left(2\pi \frac{k + \frac{n}{2}}{n}\right) \\ &= e^{i2\pi \frac{k + \frac{n}{2}}{n}} \in R_n \end{aligned}$$

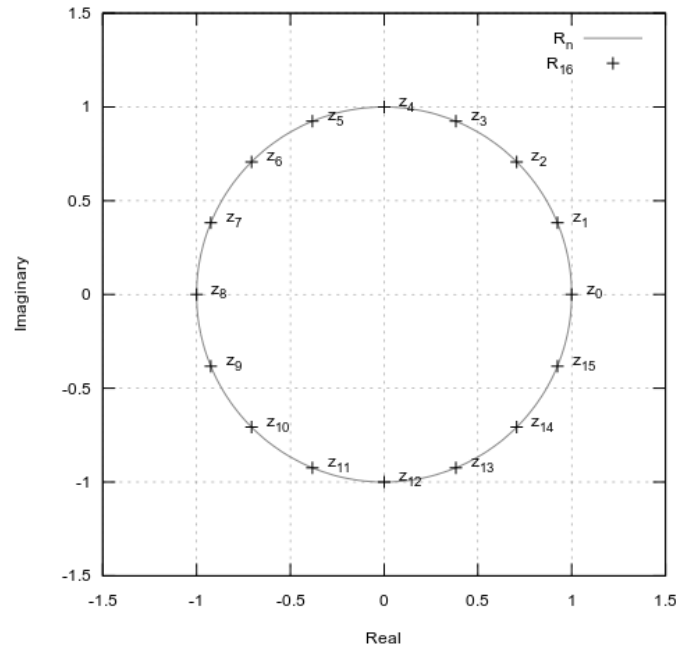
See Figure 3 that exemplifies relation (23) for $n = 16$.

$$\forall x \in R_{2^m} \ x^{2^h} \in R_{2^{m-h}} \mid h \in \mathbb{N}; h < m \quad (24)$$

Proof:

$$\begin{aligned} x^{2^h} &= \left(e^{i2\pi \frac{k}{2^m}}\right)^{2^h} = e^{i2\pi \frac{k \cdot 2^h}{2^m}} \\ &= e^{i2\pi \frac{k}{2^{m-h}}} \in R_{2^{m-h}} \end{aligned}$$

Figure 3: The R_{16} Set



Relations (23) and (24) imply that the problem of evaluating a polynomial $A(x)$ of degree $2^m - 1$, for points $x \in$

$R_{2^m} \forall m \in \mathbb{N}^*$, is reduced to the recursive evaluation of two polynomials, $A_1(x^2)$ and $A_2(x^2)$, where $x^2 \in R_{2^{m-1}}$, as such:

$$\begin{aligned} A(x) &= a_0 + a_1x + a_2x^2 + \dots + a_{2^m-1}x^{2^m-1} \\ &= (a_0 + a_2x^2 + \dots + a_{2^m-2}x^{2^m-2}) + (a_1x + a_3x^3 + \dots + a_{2^m-1}x^{2^m-1}) \\ &= (a_0 + a_2x^2 + \dots + a_{2^m-2}x^{2^m-2}) + x(a_1 + a_3x^2 + \dots + a_{2^m-1}x^{2^m-2}) \\ &= A_1(x^2) + xA_2(x^2) \end{aligned}$$

In other words:

$$\begin{aligned} A(x) &= \sum_{k=0}^{2^m-1} a_k x^k \\ &= \sum_{k=0}^{2^{m-1}-1} a_{2k} x^{2k} + \sum_{k=0}^{2^{m-1}-1} a_{2k+1} x^{2k+1} \\ &= \sum_{k=0}^{2^{m-1}-1} a_{2k} x^{2k} + x \sum_{k=0}^{2^{m-1}-1} a_{2k+1} x^{2k} \\ &= A_1(x^2) + xA_2(x^2) \end{aligned} \tag{25}$$

Moreover, we deduce that the polynomial $A(x')$ can be evaluated using the same two polynomials, $A_1(x^2)$ and $A_2(x^2)$:

$$\begin{aligned} A(x') &= A_1(x'^2) + x'A_2(x'^2) \\ &= A_1(x^2) - xA_2(x^2) \end{aligned} \tag{26}$$

Knowing (25) and (26), the following recursive solution is proposed for evaluating a polynomial $A(x)$ of degree $2^m - 1$ for all $x \in R_{2^m} \forall m \in \mathbb{N}^*$. For readability, the notation $2^m = n$ is used:

1. The task is divided into the evaluation of p and q .
2. Evaluating q requires minimal processing power once p is evaluated.
3. Evaluating p is synonymous to the evaluation of two polynomials, $A_1(x)$ and $A_2(x)$ of degree $2^{m-1} - 1$, for all values $x \in R_{2^{m-1}}$. The two evaluations are less difficult instances of the initial task, thus recurrence ensues.

Remark: This solution has a complexity of $O(n \log_2 n)$.

$$\begin{cases}
 p \begin{cases}
 A(x_0) &= A_1(x_0^2) &+ & x_0 A_2(x_0^2) \\
 A(x_1) &= A_1(x_1^2) &+ & x_1 A_2(x_1^2) \\
 \vdots & \vdots & \vdots & \vdots \\
 A\left(x_{\frac{n}{2}-1}\right) &= A_1\left(x_{\frac{n}{2}-1}^2\right) &+ & x_{\frac{n}{2}-1} A_2\left(x_{\frac{n}{2}-1}^2\right)
 \end{cases} \\
 q \begin{cases}
 A\left(x_{\frac{n}{2}}\right) &= A_1(x_0^2) &- & x_0 A_2(x_0^2) \\
 \vdots & \vdots & \vdots & \vdots \\
 A(x_{n-2}) &= A_1\left(x_{\frac{n}{2}-2}^2\right) &- & x_{\frac{n}{2}-2} A_2\left(x_{\frac{n}{2}-2}^2\right) \\
 A(x_{n-1}) &= A_1\left(x_{\frac{n}{2}-1}^2\right) &- & x_{\frac{n}{2}-1} A_2\left(x_{\frac{n}{2}-1}^2\right)
 \end{cases}
 \end{cases}$$

3.2 Matrix Reformulation

The following product between a quadratic matrix and a column vector can be evaluated through the recursive

$$\begin{bmatrix} A(\omega^0) \\ A(\omega^1) \\ A(\omega^2) \\ \vdots \\ A(\omega^{n-1}) \end{bmatrix} = \begin{bmatrix} \omega^{0\cdot0} & \omega^{0\cdot1} & \omega^{0\cdot2} & \dots & \omega^{0(n-1)} \\ \omega^{1\cdot0} & \omega^{1\cdot1} & \omega^{1\cdot2} & \dots & \omega^{1(n-1)} \\ \omega^{2\cdot0} & \omega^{2\cdot1} & \omega^{2\cdot2} & \dots & \omega^{2(n-1)} \\ \vdots & \vdots & \vdots & \ddots & \vdots \\ \omega^{(n-1)0} & \omega^{(n-1)1} & \omega^{(n-1)2} & \dots & \omega^{(n-1)(n-1)} \end{bmatrix} \begin{bmatrix} a_0 \\ a_1 \\ a_2 \\ \vdots \\ a_{n-1} \end{bmatrix}$$

Given (21), it can be deduced that the discrete Fourier transform consists of such a product. Therefore, it can be evaluated with minimal complexity if the matrix involved is written according to the following rule:

$$\begin{bmatrix} \widehat{f}_a(v_0) \\ \widehat{f}_a(v_1) \\ \widehat{f}_a(v_2) \\ \vdots \\ \widehat{f}_a(v_{n-1}) \end{bmatrix} = \frac{2}{n} \begin{bmatrix} e^{-i2\pi\frac{0\cdot0}{n}} & e^{-i2\pi\frac{0\cdot1}{n}} & e^{-i2\pi\frac{0\cdot2}{n}} & \dots & e^{-i2\pi\frac{0(n-1)}{n}} \\ e^{-i2\pi\frac{1\cdot0}{n}} & e^{-i2\pi\frac{1\cdot1}{n}} & e^{-i2\pi\frac{1\cdot2}{n}} & \dots & e^{-i2\pi\frac{1(n-1)}{n}} \\ e^{-i2\pi\frac{2\cdot0}{n}} & e^{-i2\pi\frac{2\cdot1}{n}} & e^{-i2\pi\frac{2\cdot2}{n}} & \dots & e^{-i2\pi\frac{2(n-1)}{n}} \\ \vdots & \vdots & \vdots & \ddots & \vdots \\ e^{-i2\pi\frac{(n-1)0}{n}} & e^{-i2\pi\frac{(n-1)1}{n}} & e^{-i2\pi\frac{(n-1)2}{n}} & \dots & e^{-i2\pi\frac{(n-1)(n-1)}{n}} \end{bmatrix} \begin{bmatrix} f_0 \\ f_1 \\ f_2 \\ \vdots \\ f_{n-1} \end{bmatrix} \tag{28}$$

Relation (28) is one of the forms of the fast Fourier transform.

3.3 Consequences of Matrix Reformulation

In the context of (21), (27) and (28), the matrix reformulation of the discrete Fourier transform has the following implications on the frequencies on which the transform can be applied:

polynomial evaluation method described above. This is preferable given the low complexity of the solution.

$$\omega = e^{i2\pi\frac{1}{n}} \in R_n \mid n = 2^m; m \in \mathbb{N}^*$$

$$e^{-i2\pi v_k \frac{1}{R}} = \omega^k \quad \forall k \in \{0, 1, \dots, n-1\} \tag{27}$$

Reformulating (21), we get:

$$\begin{aligned}
 e^{-i2\pi v_k \frac{1}{R}} &= e^{-i2\pi\frac{k}{n}} \Leftrightarrow \\
 v_k &= k \frac{R}{n} \Leftrightarrow \\
 \Delta v &= v_{k+1} - v_k = \frac{R}{n}
 \end{aligned} \tag{29}$$

In conclusion, the discrete Fourier transform can be calculated efficiently when the frequencies involved are

equidistantly distributed over the spectrum described by the signal's sampling rate. Therefore, relations (29) and (19) imply that, given $n = 2^m \forall m \in \mathbb{N}^*$ readings of signal $f \in A$ which contains the basic analog signals $g_k \in E$, the fast Fourier transform determines the defining parameters $(a_k, \theta_k) \in \mathbb{R} \times \mathbb{R}$ where:

$$v_k = k \frac{R}{n} \forall k \in \left\{0, 1, \dots, \frac{n}{2} - 1\right\}$$

II. Technical Implementation

This paper demonstrates the engineering utility of the Fourier transform in the design of a protocol for data transfer through audio signals.

Axiom: Any volume of data is transmissible as $n \in \mathbb{N}^*$ parallel digital signals. For $n = 1$, the transmission is considered to be serial, not parallel.

The set of time-dependent digital signals can be defined as follows:

$$D = \{h(t) \mid h: \mathbb{R} \rightarrow \{0,1\}\}$$

Theorem: A communication channel capable of maintaining the signal $f \in A$ may be used for the transmission of n parallel digital signals if the following conditions are met:

1. Each digital signal $h_k \in D \mid k \in \{0, 1, \dots, n - 1\}$ involved modulates the amplitude of an analog signal $g_k \in E$, of known parameters (a_k, v_k, θ_k) , which is part of the signal f :

$$\begin{aligned} f(t) &= \sum_{k=0}^{n-1} g_k(t) \\ &= \sum_{k=0}^{n-1} h_k(t) a_k \cos(2\pi v_k t + \theta_k) \end{aligned}$$

2. Each digital signal $h_k \in D \mid k \in \{0, 1, \dots, n - 1\}$ involved is deductible by demodulating the amplitude of an analog signal $g_k \in E$ that is part of f , where its v_k parameter is known:

$$h_k(t) = \begin{cases} 0 & |\widehat{f}_d(v_k)| \in [0, \epsilon) \\ 1 & |\widehat{f}_d(v_k)| \in [\epsilon, \infty) \end{cases}$$

Remark: The ϵ constant defines the background noise threshold of the signal f . Any signal whose amplitude is below this threshold will be omitted. Under ideal circumstances, $\epsilon \rightarrow 0$.

4 The FFT Algorithm

See Figure 4 and Figure 5 for details on the implementation of the recursive polynomial evaluation solution on which the fast Fourier transform relies.

Figure 4: Recursive Polynomial Evaluation Algorithm

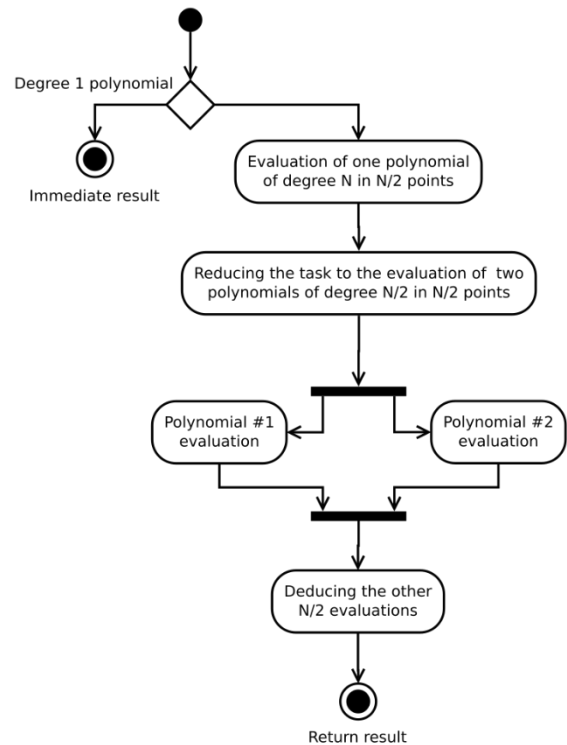


Figure 5: C++ Source Code

```
complex<long double>* fft(complex<long double>* c, complex<long double>* v,
unsigned int s)
{
    if(s == 1){
        complex<long double> *r = new complex<long double>[1];
        *r = *c; return r;
    }
    unsigned int hs = s/2;
    complex<long double> vaux;
    complex<long double> *r = new complex<long double>[s];
    complex<long double> *nv = new complex<long double>[s+hs];
    complex<long double> *c1 = nv+hs, *c2 = c1+hs;
    for(unsigned int i=0; i<hs; i++){
        vaux = v[i]; nv[i] = vaux*vaux;
        c1[i] = c[2*i];
        c2[i] = c[2*i+1];
    }
    complex<long double>* r1 = fft(c1, nv, hs);
    complex<long double>* r2 = fft(c2, nv, hs);
    for(unsigned int i=0; i<hs; i++){
        r[i] = r1[i]+v[i]*r2[i];
        r[i+hs] = r1[i]-v[i]*r2[i];
    }
    delete[] nv;
    delete[] r1;
    delete[] r2;
    return r;
}
```

5 Protocol Definition

This paper demonstrates the design of a data transfer protocol that can be attached to the command line terminal of a computer, allowing its control through processes of transmission and reception of sound signals. Consequently, the protocol is responsible for using a computer's audio interface as a control interface. For this purpose, the following are required:

1. Automatic audio interface calibration for the computers involved
2. Conversion of digital data to analog signals and vice versa
3. Identification of the computers involved
4. Possibility of performing simple, request-response transactions
5. Operation at transfer speeds of at least 64b/s
6. Simultaneous operation of independent instances of the protocol, using the same communication channel
7. Automatic detection of transfer errors

Figure 6: Transmission Diagram for n Bands

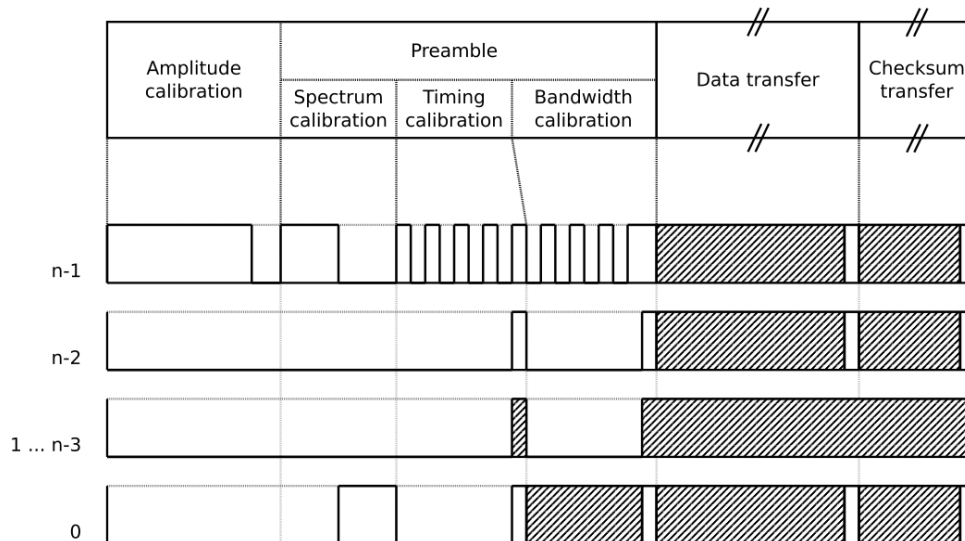


Figure 6 illustrates the segments that make up a transmission on n bands:

Amplitude Calibration: A single signal of maximum amplitude is transmitted on band $n - 1$, followed by a short pause. The beginning of a transmission is marked and the maximum amplitude used by it is communicated.

Spectrum Calibration: A single signal is transmitted on each of the bands $n - 1$ and 0 . The boundaries of the transmission's spectrum are marked.

Timing Calibration: An alternating signal is transmitted on band $n - 1$. The frequency with which the signal changes state is marked. The segment includes a terminating signal.

Bandwidth Calibration: Only bands $n - 1$ and 0 are used, their frequencies have been previously marked. The number of bands used by the data transfer is communicated in the form of a byte:

1. The signal on band $n - 1$ is a clock signal.
2. The signal on band 0 is a serial data stream.

The segment includes a terminating signal.

Data Transfer: Bands $\{0, 1, \dots, n - 1\}$ are used. An arbitrary volume of data is transmitted:

1. Signals on bands $\{n - 1, n - 2\}$ are, simultaneously, clock and control signals, see Table 1 for more details.
2. Signals on bands $\{0, 1, \dots, n - 3\}$ are a parallel data stream.

The segment includes a terminating signal.

Checksum Transfer: In the same configuration as the previous segment, the first 16 bytes of the SHA-256 checksum of the aforementioned data volume are communicated.

Figure 7: Transmission Band Assignment

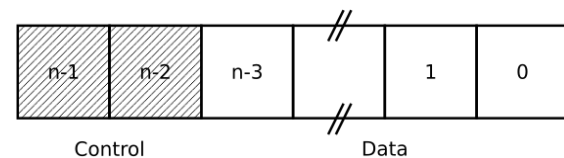


Table 1: Control Band Values

$n - 1$	$n - 2$	State
0	0	Invalid signal
0	1	Clock 0
1	0	Clock 1
1	1	Terminating Signal

Remark: Only readings of the control bands are used in detecting changes in the state of the signal.

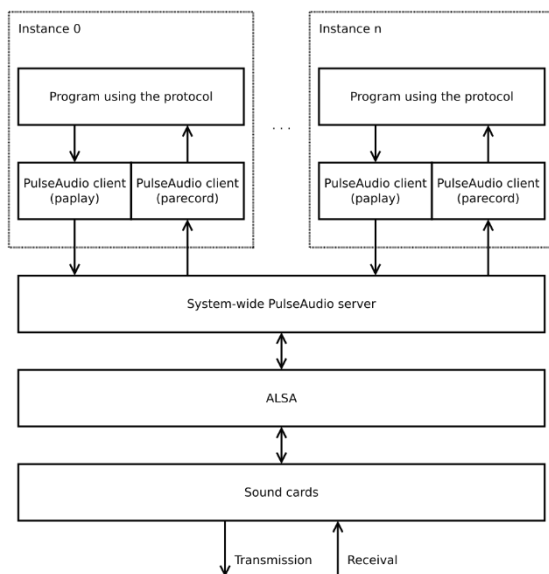
Remark: In a terminating signal, data bands with ordinal numbers {0,2,4, ...} take the value 1, the rest take the value 0.

6 Protocol Integration

6.1 Means of Transmission and Reception

Mediation between the protocol and the sound architecture of the operating system is performed by a PulseAudio server, as described in Figure 8. The PulseAudio subsystem manages the physical resources of the system and centralizes the audio streams produced by clients, allowing multiple instances of the protocol to run on a single sound card without interference.

Figure 8: PulseAudio Integration



6.2 System Service Integration

The protocol is implemented in the form of two programs:

- A. **emt** Protocol client. Transmits commands to a computer running the emtd program and waits for a response in the form of a transmission containing the output data of the commands.
- B. **emtd** Protocol server. Receives commands sent by a computer running the emt program, executes commands as the user responsible for invoking the program and responds in the form of a transmission containing the output data of the commands.

A complete description of the usage of the two programs can be found in the manual with which they are distributed, accessible through the following commands:

```
man emt
man emtd
```

The server utility can be integrated as a system service managed by GNU **systemd** [3]. This way, a command line terminal will become available through a sound card every time the system is turned on. See Figure 9 for details.

Figure 9: Configuration for emt@.service

```
[Unit]
Description=Terminal running on %I
Documentation=man:emtd(8)
BindsTo=pulseaudio.service
After=pulseaudio.service

[Service]
User=root
Type=notify
EnvironmentFile=-/run/emtd/%I
ExecStartPre=/usr/bin/emtdevparam -b -s %I
ExecStart=/usr/sbin/emtd -i $INDEX_IN -o $INDEX_OUT -m $MIN -M
$MAX -f $FREQ -b $BANDW -d $BANDS
ExecStopPost=/bin/rm -f /run/emtd/%I
Restart=on-failure
RestartPreventExitStatus=7 8
TimeoutStartSec=5

[Install]
WantedBy=multi-user.target
Alias=emtd@.service
```

Notice: The system service uses a system-wide PulseAudio instance [4], instead of a normal user instance. The configuration in Figure 9 states this requirement.

The procedure for replacing multiple PulseAudio user instances with a single system-wide PulseAudio instance is described in the **pamode** utility, distributed along with the **emt** and **emtd** programs.

III. Final Results

Figure 10 contains the QR code of the **emt-0.0-src.tar.xz** archive. It contains all that is necessary for compiling and packaging the programs mentioned in this paper using the Debian Linux format [5]. This can be done through the included sequence of commands.

Figure 10: QR Code of the Implementation



```
unxz emt-0.0-src.tar.xz;
tar -xf emt-0.0-src.tar;
cd emt-0.0-src/emt-0.0/;
sudo debuild;
```

7 Testing

Figure 11: Physical Connection Between a Dell E6410 (2011) and a Dell D630 (2007)



Notice: The sound cards of the two computers are connected by 3.5mm audio cables. The protocol works using any means of bidirectional transfer of the audio signal: cable, radio, telephony, recording and playback, etc.

Figure 12: Connection Procedure and the Transmission of a Command

```

edward@edward-Latitude-E6410: ~
File Edit View Search Terminal Help
edward@edward-Latitude-E6410:~$ emt $(entdevaran -b) -f 1050 -b 1900 -d 22 -I -
A 1
ent: Bandwidth allocation: 1125-2700Hz -- 22 bands
ent: Notice: Recommended baud interval: 159ms -- 137 bits/s
ent: Running server identification procedure. Please stand by.
ent: User: root
ent: Node: edward-Latitude-D630
[ent://root@edward-Latitude-D630]$ lsblk
ent: [Transmission incoming.]
ent: Base frequency: 1125Hz
ent: Average amplitude: 0.0467214
ent: Bandwidth markers: OK
ent: Timing markers: OK
ent: Bandwidth allocation: 1125-2850Hz -- 22DATA+2CTRL
ent: Estimated transfer rate: 209 bits/s
ent: [Data stream incoming.]
NAME MAJ:MIN RM SIZE RO TYPE MOUNTPOINT
sda 0:0 0 232.9G 0 disk
├─sda1 0:1 0 116.5G 0 part
├─sda2 0:2 0 1K 0 part
├─sda5 0:5 0 116.5G 0 part /
sro 1:0 1 1024M 0 rom
ent: [CHECKSUM OK]
[ent://root@edward-Latitude-D630]$
    
```

Figure 13: Transfer Error Detection and Automatic Retransmission

```

edward@edward-Latitude-E6410: ~
File Edit View Search Terminal Help
100 systemd-network 0 0 1 systemd Network Managen
t,,,
101 systemd-resolve 1 0 1 system Resolver,,,
102 syslog 1 0 1
103 messagebus 1 0 1
104 apt 0 0 1
105 uuidd 0 0 1
106 lightdm 0 0 1 Light Display M[bad]
107 whoopsie 1 0 1
108 kernoops 2 0 1 Kernel Oops Tracking Dao
,,,
109 pulse 1 0 1 PulseAudio daemon,,,
110 avahi 2 0 1 Avahi mDNS daemon,,,
111 hplip 0 0 1 HPLIP system user,,,
112 geoclue 0 0 1
011 nx 2 0 1
1000 edward 31 0 0 22:39 Edward,,,
05534 nob dp 0 0 1 nobody
ent: Error: Transmission attempt 2/4 failed with code 6.
ent: [Transmission incoming.]
ent: Base frequency: 1125Hz
ent: Average amplitude: 0.0467207
ent: Bandwidth markers: OK
ent: Timing markers: OK
    
```

Figure 14: Non-interactive Usage

```

edward@edward-Latitude-E6410: ~
File Edit View Search Terminal Help
edward@edward-Latitude-E6410:~$ while(true); do emt $(entdevaran -b) -f 1050 -b
1900 -d 22 -I -A 1 -- "ifconfig" 2> /dev/null && break; done;
enp950: flags=4099<UP,BROADCAST,MULTICAST> mtu 1500
ether 00:1c:23:06:1a:49 txqueuelen 1000 (Ethernet)
RX packets 0 bytes 0 (0.0 B)
RX errors 0 dropped 0 overruns 0 frame 0
TX packets 0 bytes 0 (0.0 B)
TX errors 0 dropped 0 overruns 0 carrier 0 collisions 0
device interrupt 17

lo: flags=73<UP,LOOPBACK,RUNNING> mtu 65536
inet 127.0.0.1 netmask 255.0.0.0
inet6 ::1 prefixlen 128 scopeid 0x10<host>
loop txqueuelen 1000 (Local Loopback)
RX packets 396 bytes 28866 (28.8 KB)
RX errors 0 dropped 0 overruns 0 frame 0
TX packets 396 bytes 28866 (28.8 KB)
TX errors 0 dropped 0 overruns 0 carrier 0 collisions 0

wlp12s0: flags=4163<UP,BROADCAST,RUNNING,MULTICAST> mtu 1500
inet 192.168.1.11 netmask 255.255.255.0 broadcast 192.168.1.255
inet6 fe80::ecc3:9e5d:5a3b:309c prefixlen 64 scopeid 0x20<link>
inet6 2a02:2f04:d406:9b00:ae8e:b4c4:36bb:d6dd prefixlen 64 scopeid 0x0
<global>
inet6 2a02:2f04:d406:9b00:8800:3067:884d:508b prefixlen 64 scopeid 0x0
<global>
ether 00:1c:bf:32:84:16 txqueuelen 1000 (Ethernet)
RX packets 3378 bytes 536339 (536.3 KB)
RX errors 0 dropped 0 overruns 0 frame 0
TX packets 380 bytes 46631 (46.6 KB)
TX errors 0 dropped 0 overruns 0 carrier 0 collisions 0

edward@edward-Latitude-E6410:~$
    
```

Notice: Invoking the **emt** program inside an infinite loop broken only by a return code of 0, as shown above, results in reattempting communication every time an

error occurs. This procedure is useful in writing non-interactive scripts.

Figure 15: Runtime Log of Receiving a Message

```

root@edward-Latitude-D630: /home/edward
File Edit Tabs Help
mar 03 21:07:37 edward-Latitude-D630 emtd[1530]: Debug: Digital band scan: #|
mar 03 21:07:37 edward-Latitude-D630 emtd[1530]: Debug: Binary frame: [10000000000000000000]
mar 03 21:07:37 edward-Latitude-D630 emtd[1530]: Debug: Decoded bytes:
mar 03 21:07:38 edward-Latitude-D630 emtd[1530]: Debug: Digital band scan: #|
mar 03 21:07:38 edward-Latitude-D630 emtd[1530]: Debug: Digital band scan: #|
mar 03 21:07:38 edward-Latitude-D630 emtd[1530]: Debug: Digital band scan: #|
mar 03 21:07:38 edward-Latitude-D630 emtd[1530]: Debug: Binary frame: [0100010110011000000000]
mar 03 21:07:38 edward-Latitude-D630 emtd[1530]: Debug: Decoded bytes:
mar 03 21:07:38 edward-Latitude-D630 emtd[1530]: Debug: Digital band scan: ##|
mar 03 21:07:38 edward-Latitude-D630 emtd[1530]: Debug: Digital band scan: ##|
mar 03 21:07:38 edward-Latitude-D630 emtd[1530]: Debug: Digital band scan: ##|
mar 03 21:07:38 edward-Latitude-D630 emtd[1530]: Debug: Digital band scan: ##|
mar 03 21:07:38 edward-Latitude-D630 emtd[1530]: Debug: Binary frame: [11010101010101010101]
mar 03 21:07:38 edward-Latitude-D630 emtd[1530]: Debug: Digital band scan: #|
mar 03 21:07:38 edward-Latitude-D630 emtd[1530]: Debug: Digital band scan: #|
mar 03 21:07:38 edward-Latitude-D630 emtd[1530]: Debug: Digital band scan: #|
mar 03 21:07:38 edward-Latitude-D630 emtd[1530]: Debug: Digital band scan: #|
mar 03 21:07:38 edward-Latitude-D630 emtd[1530]: Debug: Binary frame: [10110100110011101010]
mar 03 21:07:38 edward-Latitude-D630 emtd[1530]: [318 blob data]
mar 03 21:07:38 edward-Latitude-D630 emtd[1530]: Debug: Digital band scan: #|
mar 03 21:07:38 edward-Latitude-D630 emtd[1530]: Debug: Digital band scan: #|
    
```

Notice: Each log entry displays the determined state of the signal. This diagnostic data is not displayed on screen, instead it remains in memory and can be read by the **journalctl** program, part of **GNU systemd**.

IV. References

[1] WolframAlpha LLC, "Fourier Series", Retrieved 25 February 2022 <https://mathworld.wolfram.com/FourierSeries.html>

[2] WolframAlpha LLC, "Nyquist Frequency", Retrieved 25 February 2022 <https://mathworld.wolfram.com/NyquistFrequency.html>

[3] FreeDesktop Organisation, "systemd.service", Retrieved 26 February 2022 <https://www.freedesktop.org/software/systemd/man/systemd.service.html>

[4] FreeDesktop Organisation, "Running PulseAudio as System-Wide Daemon", Retrieved 20 February 2022 <https://www.freedesktop.org/wiki/Software/PulseAudio/Documentation/User/SystemWide/>

[5] Debian Organisation, "Chapter 4. Simple Example", Retrieved 24 February 2022 <https://www.debian.org/doc/manuals/debmake-doc/ch04.en.html>

Theoretical Aspects on Ponderomotive Forces

Dr. Mircea Ignat, MEng., Coordinator of the "Alexandru Proca" Center for the Youngsters Initiation in Scientific Research (CICST)

National Institute for Research and Development in Electrical Engineering ICPE-CA (INCDIE ICPE-CA)
Splaiul Unirii, No. 313, District 3, 030138, Bucharest, Romania
mircea.ignat@icpe-ca

Abstract - The paper proposes a theoretical study on the theorem of ponderomotive force (in electrostatic and magnetic field) with the aim of the identification the new unconventional actuation force, either the direct relations between the electrostatic and magnetic relation or use the isotropy and anisotropy of materials. Also, we present the condition of discontinuity permittivity and permeability of subdomains as the actuation effects.

Index Terms - ponderomotive, force, electrostatic, magnetic field, electromechanical actuation, permittivity, discontinuity.

I. INTRODUCTION

The theorem of the ponderomotive actions on the electrostatic field and on magnetic field [1-3] represent the main theoretical relations of the electromechanical actuations and actuators [4-6].

The form of this theorems are [1-3]:

- Theorem of the ponderomotive forces in electrostatic field

$$\begin{aligned} \bar{f}_{el} = \rho_v \bar{E} - \frac{E^2}{2} grad \varepsilon \\ + \frac{1}{2} grad \left(E^2 \frac{\partial \varepsilon}{\partial \tau} \right) \end{aligned} \quad (1)$$

- Theorem of the ponderomotive forces in magnetic field

$$\begin{aligned} \bar{f}_m = \bar{J} \times \bar{B} - \frac{1}{2} H^2 grad(\mu) \\ + \frac{1}{2} grad \left(B^2 \frac{\partial \mu}{\partial \tau} \right) \end{aligned} \quad (2)$$

where: ρ_v – volum density of electric chрге, \bar{E}, \bar{D} – electric field intensity and electric induction \bar{H}, \bar{B} – magnetic field intensity and magnetic induction, ε – electric permittivity of the medium where act the ponderomotive forces, μ – medium permeability where act the ponderomotive forces mediului, τ – mass density.

The explicit forms of the relations (1), (2) are:

$$\bar{f}_e = \bar{f}_{es} + \bar{f}_{ep} + \bar{f}_{els} \quad (3)$$

$$\bar{f}_m = \bar{f}_L + \bar{f}_{m\mu} + \bar{f}_{mms} \quad (4)$$

where \bar{f}_{es} – electric force volume density because of the electric volume density charge in electric field; \bar{f}_{ep} – electric force volume density when permittivity is a point function and is independent of electric field orientation (piezoelectric actuation), \bar{f}_{els} – electric force volume density in the case when permittivity is a mass function (electrostrictive actuation), \bar{f}_L – Lorentz force volume density, $\bar{f}_{m\mu}$ – magnetic force volume density when permeability is a point function, \bar{f}_{mms} – magnetic force volume density when permeability is a function of the mass density (magnetostriction actuation).

In Table 1, it is presented a synthetic situation on the electromechanical actuation field.

Table 1

The electro-mechanical actuation	Research field preoccupations	Applications	Commentaries
Piezoelectric	*	****	
Magneto-strictive	****	**	Subdomain (niche) important both for research and applications
Electro-striction	****	**	Subdomain important both for research and applications
Electro-magnetic (electro-dynamics)	***	***	Subdomain (niche) important both for research and applications
Electro-thermics	**	**	Subdomain (niche) important both for research and applications
Electro-statics	***	**	Subdomain (niche) important for research (MEMS)
Electro-chemical	**	*	Subdomain (niche) important for research (MEMS)
Lorentz Force	****	*	Subdomain (niche) important for research

Legend: *weak interest; ****very important interest. The tendency is indicated with arrows.

From Table 1, there are clear the tendencies in the field research and the application fields for each the electromechanical actuation types.

An essential theoretic study of the identification of the new niches in research and applications implicates the followings main electromagnetic field theorems and laws [1-3]:

- The general laws;
- The material laws;
- The ponderomotive laws in electrostatics and stationary magnetic field.

II. A THEORETICAL STUDY TO IDENTIFICATE THE NEW ACTUATION FORCES

An electromechanical actuator can be defined [4, 6] as an electromechanical conversion system which realizes a drive electromotion control of the parameters; linear or angular displacement, speed and acceleration (see Fig.1).

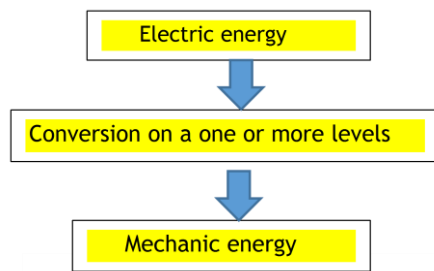


Fig. 1. The actuator as a conversion system

More levels represent: electrothermic conversion level, electrochemical conversion level etc. or succession of this conversion types.

A first analysis or theoretal study, it is accomplished on the theorem of the ponderomotive forces in electrostatic field (see relations (1) and (3)).

We consider in Table 2, an analysis of those three electrostatics forces (with the simplification and shortening form of the forces) with the possible or potential between themselves.

Table 2. A synthetic analysis of the interaction ponderomotive electrostatics forces

	$\overline{f_{es}}$	$\overline{f_{ep}}$	$\overline{f_{els}}$
$\overline{f_{es}}$	$\overline{f_{ess}}$	$\overline{f_{esp}}$	$\overline{f_{est}}$
$\overline{f_{ep}}$	$\overline{f_{esp}}$	$\overline{f_{epp}}$	$\overline{f_{ept}}$
$\overline{f_{els}}$	$\overline{f_{est}}$	$\overline{f_{ept}}$	$\overline{f_{ell}}$

In this way, we obtain still 3 distinct hybrid

actuation forces (the distinct force is to the crossing of a line force with a column force), down we consider the interaction with the vector addition:

$$\overline{f_{esp}} = \overline{f_{ep}} + \overline{f_{es}} \tag{5}$$

$$\overline{f_{est}} = \overline{f_{els}} + \overline{f_{es}} \tag{6}$$

$$\overline{f_{ept}} = \overline{f_{els}} + \overline{f_{ep}} \tag{7}$$

However, this interaction can be also multiplicative. On the matrix diagonal, the forces are not distinct. Similarly, in the case of the ponderomotive forces in magnetic field we obtain the Table 3.

Table 3. A synthetic analysis of the interaction ponderomotive magnetic forces

	$\overline{f_L}$	$\overline{f_{m\mu}}$	$\overline{f_{mms}}$
$\overline{f_L}$	$\overline{f_{Lu}}$	$\overline{f_{L\mu}}$	$\overline{f_{mLs}}$
$\overline{f_{m\mu}}$	$\overline{f_{\mu L}}$	$\overline{f_{m\mu\mu}}$	$\overline{f_{m\mu s}}$
$\overline{f_{mms}}$	$\overline{f_{m sL}}$	$\overline{f_{ms}}$	$\overline{f_{mss}}$

The next list includes the magnetic distinguish the actuation force:

$$\overline{f_{L\mu}}, \overline{f_{mLs}}, \overline{f_{m\mu s}}$$

Similarly, it is possible to show the new actuation hybrid forces among the interaction of the electrostatic forces and the magnetic forces (which appear in the relation of the ponderomotive forces), see Table 4.

Table 4. A synthetic analysis of the interaction ponderomotive magnetic forces

	$\overline{f_{es}}$	$\overline{f_{ep}}$	$\overline{f_{els}}$
$\overline{f_L}$	$\overline{f_{esL}}$	$\overline{f_{epL}}$	$\overline{f_{elsL}}$
$\overline{f_{m\mu}}$	$\overline{f_{m\mu es}}$	$\overline{f_{m\mu L}}$	$\overline{f_{elsm\mu}}$
$\overline{f_{mms}}$	$\overline{f_{esmms}}$	$\overline{f_{epmms}}$	$\overline{f_{elsL}}$

In this case, all the force of the matrix of Table 4 can be considered news.

Through this study are identified 15 new actuation forces: 3 electrostatic forces, 3 magnetic forces and 9 hybrid forces!

III. OTHER NECESSARY LAWS

In the electromechanical actuation theory [4, 5, 7-11], others general laws [1-3] interfere that cannot neglect, because is not possible to comprehend the functional mechanisms of the actuation:

- the laws with direct implication: electrolysis law,
- the law of magnetic circuit,
- the law of energy transformation on the electric conductors, etc.,
- the laws with indirect implication;
- the law of electric conduction,
- the law of temporary electric polarization,
- the law of temporary magnetic polarization, etc.

For example, the differential form of the electrolysis law:

$$\frac{dm}{dt} = \frac{Ai}{n_v F_0} \quad (8)$$

where: i - the electric current, m - the fall out mass to the electrochemical process, A - the atomic mass, n_v - the element valence, F_0 - the Faraday ratio.

An electrochemical actuator, which function on the electrolysis law, has the simple conversion in Fig. 2.

$$Q = UIt [J] \quad (9)$$

This heating energy produces the linear surface or volume dilatation and the actuation conversion is presented in Fig. 3.

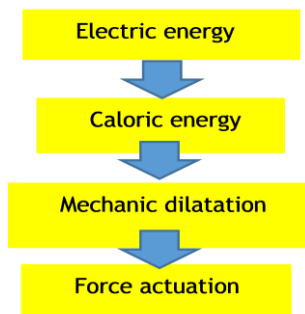


Fig. 3. The conversion of the electrothermic actuator

An example of the electrothermic actuator is the thermal relay [5].

Another important actuation force is the Laplace force (electromagnetic force) [1-3]. The Laplace formula is:

$$d\vec{F}_L = i\vec{dl} \times \vec{B} \quad (10)$$

The formula represents the force acting on a current element idl in a magnetic field of a magnetic induction \vec{B} .

If we integrate we obtain:

$$\vec{F}_l \int_C d\vec{F}_L = i \int_C \vec{dl} \times \vec{B} \quad (11)$$

The electromagnetic force has different forms [12], among very important is the force between two conductors with length l and distance a which are crossed by the electric currents, i_1, i_2 [13]:

$$F_{li} = 2i_1i_2 \frac{l}{a} \varphi\left(\frac{a}{l}\right) 10^{-7} [N] \quad (12)$$

In Fig. 4, there are presented some structures of electromagnetic actuation based on the Laplace (electromagnetic) force.

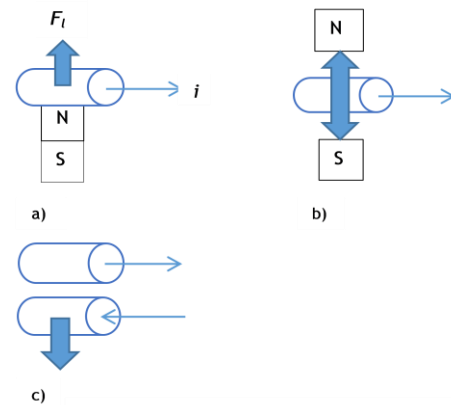


Fig. 4. Different structures of electromagnetic actuation

In Fig. 4, the structures include an electric conductor and a permanent magnet to outward side (a), an electric conductor between two permanent conductor (b), and two electric conductor with two opposite currents (c).

IV. AN ANALYSIS OF THE PONDEROMOTIVE FORCES IN ELECTROSTATIC FIELD

The analysis begins with the first term of the relation (1):

$$\vec{f}_{es} = \rho_v \vec{E} \quad (13)$$

where \vec{f}_{es} - electric force volume density because of the electric volume density charge in electric field.

A relation between the conductivity and resistivity is:

$$\sigma_v = \frac{1}{\rho_v} \quad (14)$$

and a tensor expression in anisotropy condition:

$$\frac{1}{\bar{\sigma}} = \bar{\rho}_v \quad (15)$$

with a tensor description [2, 3]:

$$\bar{\sigma}_v = \begin{pmatrix} \sigma_{xx} & \sigma_{xy} & \sigma_{xz} \\ \sigma_{yx} & \sigma_{yy} & \sigma_{yz} \\ \sigma_{zx} & \sigma_{zy} & \sigma_{zz} \end{pmatrix} \quad (16)$$

which can indicate other electromechanical actuation types with different force on each axis, as in Fig. 5, function by the resistivity (conductivity):

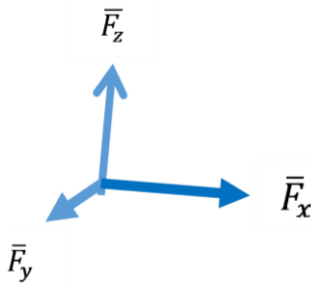


Fig. 5. The different force (anisotropic force) on each axis

Thus, is possible to speak on materials with different actuation behavior (displacement, speed, force) to each axis.

Another main analysis is for \bar{f}_{ep} - electric force volume density in the case when permittivity is a point function and is independent of electric field orientation (piezoelectric actuation):

$$\bar{f}_{ep} = -\frac{E^2}{2} grad(\varepsilon) \quad (17)$$

where according to the mathematic rules [1, 2, 13, 14]:

$$grad(\varepsilon) = \lim \frac{\int_S \varepsilon dA}{V}_s \quad (18)$$

$$grad(\varepsilon) = \nabla \varepsilon = \bar{i} \frac{\partial \varepsilon}{\partial x} + \bar{j} \frac{\partial \varepsilon}{\partial y} + \bar{k} \frac{\partial \varepsilon}{\partial z} \quad (19)$$

where S is the surface which closes the volume V_s , \bar{dA} the surface element vector, and P - point.

If ε is constant, then $grad(\varepsilon) = \mathbf{0}$ and explicit the $\bar{f}_{ep} = \mathbf{0}$.

In this way, the electric permittivity of the domain has a variable distribution and the vector $grad \varepsilon$ can be represented as in Fig. 6.

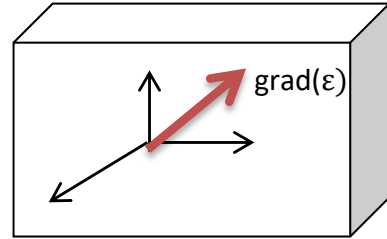


Fig. 6. A representation of $grad(\varepsilon)$ on a dielectric domain

In the same idea, an analysis of the electrostrictive force:

$$\bar{f}_{els} = \frac{1}{2} grad \left(E^2 \frac{\partial \varepsilon}{\partial \tau} \right) \quad (20)$$

where $\frac{\partial \varepsilon}{\partial \tau}$ appears as the partial differential, also it means that a permittivity variation (even the discontinuities problems) requires a distinct commentary in the purpose to identify the new the new electromechanical actuation functional effects and structures.

So, we can see the permittivity has main distribution variation or discontinuities, we say about same distinct actuation structures (see Fig. 7).

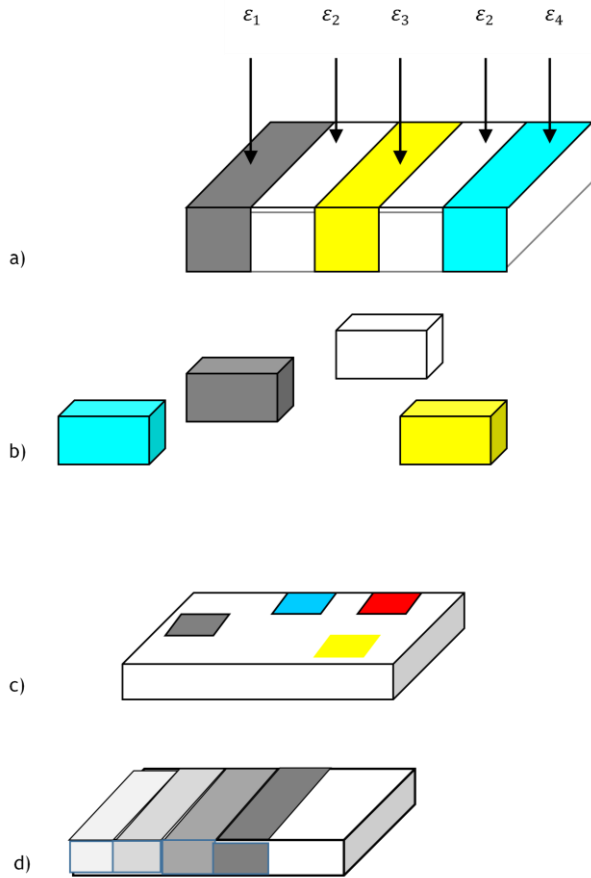


Fig. 7. The different electromechanical actuation structures

In Fig. 7a), it is presented a succession of piezoelectric blades with different electric permittivity for a linear actuation, the separates element with different permittivity for dominoes actuation structures are presented in Fig. 7b), a mosaic structure is showed in Fig. 7c), and a progressive structure of permittivity is included in Fig. 7d).

V. DISCUSSION

The analysis of theorem of ponderomotive forces in electrostatic field and the theorem of ponderomotive forces in magnetic field (see Tables 2, 3, and 4), distinguishes 15 new actuation forces: 3 electrostatic forces, 3 magnetic forces and 9 hybrid forces, potential actuation functional effects. This potential actuation forces is extended with the thermic and electrochemical actuation functional effects.

Another source for an innovating landing are the structure of the actuation and the electromechanical actuators [4, 8, 10].

A theoretical and experimental interesting study is represented by the surface discontinuity between different subdomains of the actuation

structure, as in Fig. 8 where there are 3 distinct subdomain in the main support of actuation:

$$\begin{aligned} &\Omega_1(\varepsilon_1, \tau_1), \\ &\Omega_2(\varepsilon_2, \tau_2), \\ &\Omega_3(\varepsilon_3, \tau_3). \end{aligned}$$

Each subdomain with different main parameters, as for instance permittivity and mass density. Therefore, it can appears to the discontinuity surface the, two independent electromechanical force actuation.

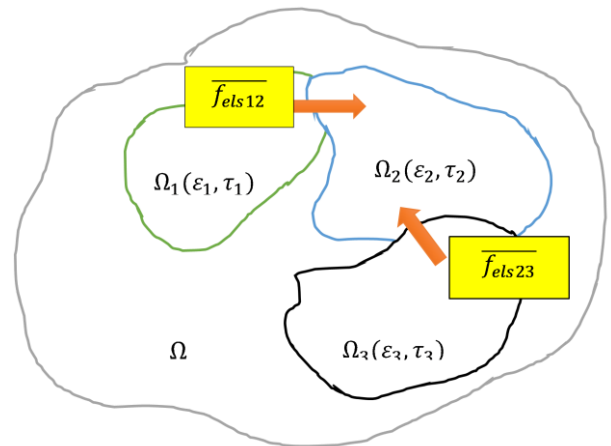


Fig. 8. An actuation structure with two independent actuation force

However, the identification of the new unconventional actuation forces and functional effects is not possible without the collaboration of the material specialists.

VI. CONCLUSIONS

The paper proposes a theoretical mode, or way, to identify the unconventional actuation force developed by the theorem of the ponderomotive force in electric field and the theorem of the ponderomotive force in magnetic field and the relation among this force, for the hybrid actuation structures.

Certainly that is necessary a critical analysis for to know and to select or to choose the efficiency actuation forces.

VIII. REFERENCES

- [1] Nicolaide A., "Electromagnetics. General Theory of the electromagnetic field", Transylvania University Press, Brasov, 2009.
- [2] Mocanu C.I., "Teoria câmpului electromagnetic", Editura Didactică și pedagogică, București, 1984.
- [3] Timotin s.a., "Lección de bazele electrotehnicii", Editura Didactica și Pedagogică, 1962.

- [4] Tai Run Hsu, „MEMS and Microsystems. Design. Manufacture and Nanoscale Engineering”, John Wiley&Sons, New Jersey, 2008.
- [5] Ignat M., Amza Gh., Haraguta Cr., “Actuatori electromecanici neconventionali”, Ed. Electra, 2003.
- [6] Ignat M., “Micromotoare și microactuatori piezoelectrice”, Ed. Electra, 2005.
- [7] Wissler M.T., “Modelling Dielectric Elastomer Actuators”, Dissertation for the degree of Doctor in Science (DISS.ETH No.17142), Swiss Federal Institute of Technology in Zurich, 2007.
- [8] Carpi F., De Rossi D., Kornbluh R., Pelrine R., Larsen P.S., „Dielectric Elastomers as Electromechanical Transducers”, Elsevier, 2007
- [9] Goranovic G., “Electrodynamic aspects of two–fluid microfluidic systems: theory and simulation”, PhD. Thesis, no.000699, Mikroelektronik Centre, Technical University of Denmark, 15 august 2003.
- [10] Pelesko J.A., Bernstein D.H., “Modelling MEMS”, Chapman, Hall/CRC, Press Company, London, New York, 2003.
- [11] Murphy N., “Introduction to Magnetohydrodynamics”, Harvard-Smithsonian Center for Astrophysics, July 6, 2012.
- [12] Ignat M., Puflea I., Pâslaru Dănescu L., “Actuatori electromagnetici”, Ed. Electra, 2006.
- [13] Hortopan Gh., Aparate electrice, Ed. Didactica si Pedagogica, 1986.

- [14] Roșculeț M., Analiza matematică, Vol. I, II, Ed. Didactică și Pedagogică, 1967.
- [15] Șabac I. Gh. Matematici speciale, Vol. I, II, Ed. Didactică și Pedagogică, 1965.

VI. BIOGRAPHY

Mircea IGNAT was born in Bucharest (Romania), on March 4, 1953.

He graduated the Politehnica University, Faculty of Electrical Engineering in Bucharest (Romania), in 1977.

He received the PhD degree in electrical engineering from the Politehnica University of Bucharest, in 1999.



He is Senior Researcher of INCDIE ICPE-CA, Bucharest.

His research interests concern: unconventional electric machines, electromechanical actuators, and medical engineering.

INDEX of AUTHORS

		Page numbers
A		
Albei	Victor-Eduard	7, 19
I		
Ignat	Mircea	33

